

1 **Enhanced hemato-endothelial specification during human embryonic differentiation**  
2 **through developmental cooperation between *AF4-MLL* and *MLL-AF4* fusions**

3  
4 Clara Bueno<sup>1,6\*</sup>, Fernando J Calero-Nieto<sup>2</sup>, Xiaonan Wang<sup>2</sup>, Rafael Valdés-Mas<sup>3</sup>,  
5 Francisco Gutiérrez-Agüera<sup>1</sup>, Heleia Roca-Ho<sup>1</sup>, Veronica Ayllon<sup>4</sup>, Pedro J Real<sup>4</sup>, David Arambilet<sup>5</sup>,  
6 Lluís Espinosa<sup>5,6</sup>, Raul Torres-Ruiz<sup>1</sup>, Antonio Agraz-Doblas<sup>1,7</sup>, Ignacio Varela<sup>7</sup>, Jasper de Boer<sup>8</sup>,  
7 Anna Bigas<sup>5,6</sup>, Bertie Gottgens<sup>2</sup>, Rolf Marschalek<sup>9</sup>, Pablo Menendez<sup>1,6,10\*</sup>

8  
9  
10 <sup>1</sup>Josep Carreras Leukemia Research Institute and Department of Biomedicine, School of Medicine.  
11 University of Barcelona. Barcelona. Spain. <sup>2</sup>Department of Hematology, Cambridge Institute for Medical  
12 Research and Wellcome Trust-Medical Research Council Cambridge Stem Cell Institute, University of  
13 Cambridge, United Kingdom. <sup>3</sup>Dreamgenics S.L. Oviedo. Spain. <sup>4</sup>GENyO, Centre for Genomics and  
14 Oncological Research, Pfizer/University of Granada/Andalusian Regional Government and University of  
15 Granada, Department of Biochemistry and Molecular Biology, Granada, Spain. <sup>5</sup>Programa de Càncer.  
16 Instituto Hospital del Mar de Investigaciones Mèdicas. Barcelona. Spain. <sup>6</sup>Centro de Investigación Biomédica  
17 en Red de Càncer (CIBER-ONC), ISCIII, Barcelona, Spain. <sup>7</sup>Instituto de Biomedicina y Biotecnología de  
18 Cantabria (CSIC-UC-Sodercan), Departamento de Biología Molecular, Universidad de Cantabria, Santander,  
19 Spain. <sup>8</sup>Cancer Section, UCL Great Ormond Street Institute of Child Health, London, United Kingdom.  
20 <sup>9</sup>Institute of Pharmaceutical Biology, Goethe-University. Frankfurt. Germany. <sup>10</sup>Institució Catalana de  
21 Recerca i Estudis Avançats (ICREA). Barcelona. Spain.

22  
23 **Running Title:** AF4-MLL in human embryonic hematopoietic development

24 **Key words:** AF4-MLL, MLL-AF4, HOX cluster, human ESC, hemato-endothelial specification.

25  
26  
27  
28 **\*Correspondence should be addressed to:**

29 Clara Bueno PhD & Pablo Menendez PhD  
30 Josep Carreras Leukemia Research Institute  
31 School of Medicine. University of Barcelona.  
32 Casanova 143, 08036. Barcelona. Spain.  
33 [cbueno@carrerasresearch.org](mailto:cbueno@carrerasresearch.org) ; [pmenendez@carrerasresearch.org](mailto:pmenendez@carrerasresearch.org)

39 **ABSTRACT**

40 The t(4;11)(q21;q23) translocation is associated with high-risk infant pro-B-cell acute lymphoblastic leukemia  
41 and arises prenatally during embryonic/fetal hematopoiesis. The developmental/pathogenic contribution of  
42 the t(4;11)-resulting *MLL-AF4* (MA4) and *AF4-MLL* (A4M) fusions remains **unclear**; MA4 is always expressed  
43 in t(4;11)+ B-cell acute lymphoblastic leukemia patients, but the reciprocal fusion A4M is expressed in only  
44 half of the patients. Because prenatal leukemogenesis manifests as impaired early hematopoietic  
45 differentiation, we took advantage of well-established human embryonic stem cell-based hematopoietic  
46 differentiation models to study whether the A4M fusion cooperates with MA4 during early human  
47 hematopoietic development. Co-expression of A4M and MA4 strongly promoted the emergence of hemato-  
48 endothelial precursors, both endothelial- and hemogenic-primed. Double fusion-expressing hemato-  
49 endothelial precursors specified into significantly higher numbers of both hematopoietic and endothelial-  
50 committed cells, irrespective of the differentiation protocol used and without hijacking survival/proliferation.  
51 Functional analysis of differentially expressed genes and differentially enriched H3K79me3 genomic regions  
52 by RNA-seq and H3K79me3 ChIP-seq, respectively, confirmed a hematopoietic/endothelial cell  
53 differentiation signature in double fusion-expressing hemato-endothelial precursors. Importantly, ChIP-seq  
54 analysis revealed a significant enrichment of H3K79 methylated regions specifically associated with *HOX-A*  
55 cluster genes in double fusion-expressing differentiating hematopoietic cells. Overall, these results establish  
56 a functional and molecular cooperation between MA4 and A4M fusions during human hematopoietic  
57 development.

58

59

60

61

62

## 63 INTRODUCTION

64 The mixed-lineage leukemia (*MLL*) gene encodes for an H3K4 histone methyltransferase important in  
65 hematopoietic development<sup>1</sup>. The human *MLL* gene is frequently rearranged in acute leukemia and typically  
66 confers a dismal outcome<sup>2,3</sup>. Of particular interest is the translocation t(4;11)(q21;q23), which encodes the  
67 fusion proteins *MLL-AF4* (*MA4*) and *AF4-MLL* (*A4M*), and is associated with infant B-cell acute lymphoblastic  
68 leukemia (B-ALL). This t(4;11)+ infant leukemia is characterized by a very brief latency, raising the question  
69 of how it evolves so quickly<sup>4</sup>. Moreover, the exceptionally high concordance rate of t(4;11)+ B-ALL in  
70 monozygotic twin infants<sup>5,6</sup> suggests that all the necessary (epi)genetic events required for leukemogenesis  
71 are accomplished prenatally, during embryonic/fetal hematopoietic development<sup>7</sup>. However, our  
72 understanding of t(4;11)-mediated developmental effects is limited, at least in part, due to the variety of  
73 phenotypes and long latency observed in currently available t(4;11) mouse models<sup>2,8-17</sup>. These different  
74 phenotypes likely result from targeting a cell in the wrong developmental stage, or not addressing the impact  
75 of secondary hits, leaving open questions about the developmental impact of the t(4;11) translocation during  
76 early human development.

77

78 The functional and molecular contribution of the reciprocal fusion genes resulting from the derivative  
79 translocated chromosomes remains obscure in cancer. The MA4 fusion is always expressed in t(4;11)+B-  
80 ALL patients, whereas the reciprocal fusion A4M is expressed in only half of the patients<sup>18-20</sup>. Importantly,  
81 t(4;11)+ cell lines display addiction to MA4 but not to A4M<sup>21,22</sup>, and although A4M was not sufficient to initiate  
82 leukemia in cord blood-derived CD34+ cells<sup>23</sup>, it was nevertheless capable of initiating B-ALL in mice without  
83 the requirement of MA4, indicating that it contributes to t(4;11)-driven leukemogenesis<sup>11,24,25</sup>. Strikingly, a  
84 very recent clinical study have unraveled an independent prognostic value for MA4 expression in t(4;11)+  
85 infant B-ALL, thus adding a new piece to the puzzle<sup>19</sup>. Thus, the developmental/pathogenic contribution of  
86 the t(4;11)-resulting reciprocal fusion A4M remains enigmatic.

87 Human embryonic stem cells (hESCs) represent a powerful tool for modeling different developmental aspects  
88 of human disease that cannot otherwise be addressed by patient sample analyses or mouse models<sup>7,26,27</sup>.  
89 Because prenatal leukemogenesis manifests as impaired early hematopoietic differentiation, modeling  
90 hematopoietic differentiation in hESCs may represent a promising *in vitro* approach to study the onset of  
91 hematopoiesis and the mechanisms underlying early human hematopoietic development<sup>7</sup>. During hESC  
92 differentiation, a primitive population of CD45<sup>-</sup> hemato-endothelial precursors (HEPs) arises and further  
93 differentiates into CD45<sup>+</sup> hematopoietic and mature endothelial cells<sup>28-30</sup>. Beyond their pathogenic role in  
94 acute leukemias, the *MLL* gene has also been implicated in endothelial cell maturation<sup>31</sup>, and endothelial  
95 dysfunction was recently linked to disease outcomes in childhood leukemias<sup>32</sup>. We previously reported that  
96 MA4 favors the emergence of endothelial-primed HEPs but not hemogenic HEPs from hESCs<sup>10</sup>. Here, we  
97 took advantage of well-established hESC-based differentiation systems to study whether the A4M fusion  
98 cooperates with MA4 during early human hematopoietic and endothelial development. We report a functional  
99 and molecular cooperation between MA4 and A4M fusions, which results in an enhanced hemato-endothelial  
100 output during human embryonic development.

101

102

103

104

105

106

107

108

109

110

## 111 **METHODS**

### 112 **Vector construction and lentiviral transduction**

113 The cDNAs for MA4 and A4M were subcloned into the pRRL-EF1 $\alpha$ -PGK-NEO vector<sup>11, 16</sup>. Both fusions have  
114 been described previously (**FigS1A**)<sup>11,23</sup>. We used the following lentivectors containing either neomycin or  
115 dTo for cell selection: pRRL-EF1 $\alpha$ -PGK-NEO (empty vector;EV), pRRL-EF1 $\alpha$ -MA4-PGK-NEO (MA4) and  
116 pRRL-EF1 $\alpha$ -A4M-PGK-dTo (A4M). VSV-G-pseudotyped lentiviral particles were generated in 293T cells  
117 using standard transfection protocols and concentrated by ultracentrifugation<sup>33</sup>. hESCs were infected  
118 overnight with concentrated EV or MA4 lentivirus plus 8  $\mu$ g/ml polybrene. Viral supernatants were washed  
119 away the next day, and EV- and MA4-transduced hESCs were then selected with G418 (50-100 $\mu$ g/ml) for  
120 three weeks. For dual transduction of MA4 and A4M fusions, G418-resistant MA4-expressing hESCs were  
121 infected with A4M-expressing viruses. EV/G418-selected hESCs were also transduced with A4M alone.  
122 Transgene expression was confirmed for all the genotypes (**Fig1**).

123

### 124 **Human ESC culture and characterization of transgenic human ESC lines**

125 hESCs (AND1 line) were maintained undifferentiated on a layer of irradiated-hMSCs (iMSC) in complete KO-  
126 DMEM medium containing 20% knockout serum replacement and 8 ng/mL basic fibroblast growth factor  
127 (bFGF)<sup>34, 35</sup>. The medium was changed daily, and cells were passaged weekly by dissociation with 1:1  
128 collagenase IV:Dispase. Cultures were visualized daily by phase contrast microscopy. Approval for hESC  
129 work was obtained from the Spanish National Embryo Ethical Committee. Pluripotency of transgenic hESCs  
130 was characterized by flow cytometry using antibodies against SSEA-3, SSEA-4 TRA-1-60 and TRA-1-81 (BD  
131 Biosciences)<sup>36</sup>. Expression of the pluripotency-associated transcription factors *OCT4*, *NANOG*, *SOX2*,  
132 *CRIP1*, and *DNMT3B* as well as transgene expression (*MA4* and *A4M*) were analyzed by qRT-PCR.  
133 **TableS1** shows the primers and PCR conditions used<sup>23,37,38</sup>.

134 **Hematopoietic differentiation from human ESCs by embryoid body formation.**

135 Undifferentiated hESCs were treated with collagenase IV:Dispase for 1 hr at 37°C. For embryoid body (EB)  
136 formation, cells were transferred to low-attachment plates and incubated overnight in differentiation medium  
137 (DM; KO-DMEM supplemented with 20% FBS, 1% nonessential amino acids, 1 mmol/L L-glutamine, and 0.1  
138 mmol/L  $\beta$ -mercaptoethanol). The medium was changed next day to the same DM supplemented with the  
139 following hematopoietic cytokines: 300 ng/mL stem cell factor (SCF), 300 ng/mL Flt3L, 10 ng/mL interleukin  
140 (IL)-3, 10 ng/mL IL-6, 50 ng/mL granulocyte-colony stimulating factor (G-CSF) and 25 ng/mL bone  
141 morphogenetic protein 4 (BMP-4) (all from R&D)<sup>9,29,39-41</sup>. EBs were dissociated at different time points during  
142 development using collagenase B and enzyme-free Cell Dissociation Buffer (Invitrogen). Dissociated cells  
143 were stained with anti-CD34-PE, anti-CD31-FITC, anti-CD45-APC or anti-CD34-PE-Cy7, CD31-BV510, anti-  
144 Glycophorin A, anti-CD43-FITC, anti-CD45-APC antibodies (all from BD Biosciences) and 7-actinomycin D,  
145 and analyzed using a FACS Canto flow cytometer<sup>9,29,39-41</sup>. Colony-forming unit (CFU) assays were performed  
146 at day 10 and 15 of EB differentiation by plating  $60 \times 10^4$  EB cells onto serum-free methylcellulose H4435  
147 (Stem Cell Technologies). Colonies were scored after 12 days<sup>9,29,42-44</sup>.

148

149 **Cell cycle and apoptosis analysis**

150 For cell cycle analysis of hESC-derived HEPs and CD45<sup>+</sup> cells, day 15 EBs were dissociated and harvested  
151 cells were fixed overnight in 70% ice-cold ethanol. Cells were then washed in PBS and incubated with anti-  
152 CD31-FITC, anti-CD34-PE-Cy7 and anti-CD45-APC antibodies for 15 min. Cells were then suspended in  
153 propidium iodide-containing buffer and acquired-analysed on a FACS Canto-II using Modfit LT4.0 software,  
154 discriminating between quiescent cells (G0/G1), cycling cells (S-phase) and G2/M cells<sup>45,46</sup>. Apoptosis was  
155 assessed with the Annexin-V apoptosis detection kit (BD Biosciences)<sup>16</sup>.

156

157 **Human ESC-OP9 co-cultures**

158 hESC-OP9 co-cultures were performed as described<sup>47,48</sup>. OP9 stroma was prepared by plating OP9 cells in  
159 gelatin-coated dishes, and allowing them to overgrow as a monolayer. hESCs were prepared as a suspension  
160 of small aggregates using collagenase IV:Dispase. One-tenth of this suspension was plated on top of the 8-  
161 day overgrown OP9 stroma. Media was replaced on the next day and one-half volume media changes were  
162 performed every other day thereafter. Hematopoietic differentiation was assessed by flow cytometry at day  
163 9 of co-culture. Accordingly, hESC-OP9 co-cultures were treated with collagenase IV/TrypLE and cells were  
164 dissociated and filtered through a 70- $\mu$ m strainer. Cell suspensions were stained with anti-mouse CD29-  
165 FITC and anti-human CD34-PE and CD45-APC antibodies. The proportion of HEPs (CD34<sup>+</sup>CD31<sup>+</sup>CD45<sup>-</sup>),  
166 and total blood cells (CD45<sup>+</sup>) was analyzed within the CD29<sup>-</sup> human ESC-derived cell population. Hemogenic  
167 and endothelial HEPs were distinguished based on CD34 and CD43 expression<sup>40</sup>.

168

169 **Culture of FACS-isolated HEPs in MS5 stroma or liquid culture**

170 Day 9 human hESC-OP9 co-cultures were dissociated as above and both CD45<sup>+</sup> cells and HEPs were  
171 analyzed. FACS-purified HEPs (CD29<sup>-</sup>CD34<sup>+</sup>CD31<sup>+</sup>CD45<sup>-</sup>) were plated onto MS5 stroma or in liquid culture  
172 for 30 or 16 days, respectively, in DM with hematopoietic cytokines (50 ng/mL SCF, 50 ng/mL Flt3L, 10 ng/mL  
173 IL-3, 20 ng/mL IL-7). The medium was changed every 7 days, and the emergence of CD45<sup>+</sup> hematopoietic  
174 cells was analyzed by FACS.

175

176 **Endothelial differentiation of HEPs**

177 HEPs ( $2 \times 10^4$ ) from day 9 human hESC-OP9 co-cultures were seeded onto 0.1% gelatin-coated plates in  
178 complete EGM-2 medium with microvasculature supplements (Lonza) for 7 days. Cells were then fixed,  
179 permeabilized and stained with rabbit anti-human VE-cadherin (Cayman), mouse anti-human eNOS (BD  
180 Biosciences), and mouse anti-human vWF (DAKO) followed by Alexa488-conjugated anti-rabbit or Cy3-

181 conjugated anti-mouse (Jakson Immunoresearch) antibodies. Nuclei were counterstained with DAPI. Images  
182 were obtained using an inverted fluorescence microscope. Day 7 differentiating cells were trypsinized and  
183 cell suspensions were stained with anti-human CD31-FITC and CD144-PerCP-Cy5.5 antibodies.

184

#### 185 **Mouse transplantation and analysis of hematopoietic-endothelial engraftment**

186 NOD/LtSz-scid IL-2R $\gamma$ <sup>-/-</sup> (NSG) mice were housed under sterile conditions. The Animal Care Committee  
187 approved all mouse protocols. Briefly, cord blood-derived CD34<sup>+</sup> HSPCs (3×10<sup>4</sup> cells) or cells from day 15  
188 EBs (5×10<sup>5</sup> cells) were intra-bone marrow (BM)-transplanted as described<sup>49</sup>. Animal health was monitored  
189 throughout the entire experiment. Mice were killed 10 weeks after transplantation and cell suspensions were  
190 analyzed by FACS for human chimerism using anti-HLA-ABC-FITC, anti-CD31-PE, CD144-PerCP-Cy5.5,  
191 and anti-CD45-APC antibodies.

192

#### 193 **Statistical analysis**

194 All data are expressed as mean±SEM. Statistical comparisons were performed using the GraphPad Prism  
195 software with the nonparametric Mann-Whitney test, two-tailed P-value (95% confidence interval). Statistical  
196 significance was defined as a p-value<0.05.

197

198 **Online methods** show detailed information about RNA- and Chromatin Immunoprecipitation sequencing and  
199 analysis.

200



201 **RESULTS**

202 **Co-expression of A4M and MA4 does not hijack pluripotency**

203 We showed very recently that only 45% of t(4;11)+ B-ALL patients express the reciprocal fusion A4M,  
204 whereas MA4 is consistently expressed in all t(4;11)+ B-ALL patients (**Fig1A**)<sup>18-20</sup>. Here, we generated  
205 transgenic hESC lines expressing “MA4 alone”, “A4M alone” or MA4+A4M (double fusion, **Fig1B, S1B**). EV  
206 (control)- and MA4-hESCs were established by G418 selection<sup>9</sup>. G418-resistant EV- or MA4-expressing  
207 hESCs were then transduced with A4M/dTo-expressing lentiviruses and >90% transduction efficiency was  
208 achieved. Transgenic hESC lines were maintained for >50 passages and retained human ESC-like  
209 morphology (**Fig1B**, left), transgene expression (**Fig1B**, right), and expression of pluripotency-associated  
210 transcription factors (**Fig1C**) and surface markers (**Fig1D**). All hESC genotypes formed teratomas in NSG  
211 mice (data not shown)<sup>9, 50</sup>. Thus, (co-)expression of A4M and/or MA4 is compatible with hESC pluripotency.

212

213 **A4M and MA4 co-operate to promote HEPs emergence and enhance blood production**

214 Hematopoietic differentiation was assessed using two distinct and well-established differentiation systems:  
215 EB formation<sup>43,47</sup> (**Fig2**) and OP9 co-culture<sup>47,48</sup> (**Fig3**). During differentiation, a population of primitive HEPs  
216 arises, which is responsible for further hematopoietic and endothelial commitment<sup>10,30</sup> (**Fig2A,3A**). We  
217 investigated whether co-expression of A4M and MA4 impacts hESC-derived hematopoiesis by analyzing the  
218 emergence of HEPs during EB development in hESCs individually expressing the single fusions or the double  
219 fusion. We observed a pronounced (~5-10-fold; p<0.05) increase in HEPs at day 7 and 10 of development in  
220 EBs expressing the double A4M and MA4 fusion over single fusions (**Fig2B**, upper-left panel). We next  
221 assessed whether co-expression of A4M and MA4 influences subsequent hematopoietic commitment of  
222 HEPs. The kinetics of emergence and output of both total CD45<sup>+</sup> hematopoietic cells and CD45<sup>+</sup>CD34<sup>+</sup>  
223 hematopoietic progenitors was faster (EB day 10) from double fusion-expressing hESCs than from equivalent  
224 single fusion-expressing cells, achieving a 2-3-fold higher hematopoietic output by day 15 of EB development

225 (Fig2B). Furthermore, double fusion-expressing HEPs massively accelerated (EB day10) the emergence of  
226 clonogenic hematopoietic progenitors as compared to single fusion-expressing HEPs (Fig2B, bottom-right  
227 panel). According to our previous work, if the kinetics of hEB differentiation are extended allowing for a  
228 continuum HEP-to-blood transition, MA4-expressing hEBs display an enhanced HEP production coupled to  
229 an impaired blood output (EB day 20, Fig S2A) and clonogenic potential (EB day 15, Fig 2B). We confirmed  
230 stable expression of ectopic MA4 and A4M upon EB differentiation, supporting the link between genotype  
231 and phenotype (Fig2C).

232

233 We also investigated hematopoietic differentiation using the OP9 differentiation system (Fig3A,B), and by  
234 plating FACS-sorted HEPs in either hematopoietic liquid culture (Fig3C) or onto MS5 feeders (Fig3D). After  
235 10 days on OP9 stroma, double fusion-expressing hESCs yielded a 10-fold higher number of CD45+  
236 hematopoietic cells than did single fusion-expressing hESCs (Fig3B). Moreover, when HEPs were FACS-  
237 sorted from day 9 OP9 co-cultures and allowed to differentiate into CD45+ blood cells, the yield of CD45+  
238 cells was up to 60-fold higher in double fusion-expressing HEPs than in single fusion-expressing HEPs.  
239 (Fig3C,D). Encouraged by these results, we next investigated whether ectopic expression of both A4M and  
240 MA4 confers *in vivo* engraftment capacity to hESC-derived hematopoietic derivatives. To do this, we  
241 transplanted  $5 \times 10^5$  hESC hematopoietic derivatives from each genotype into myeloablated NSG mice<sup>4,43,47</sup>,  
242 finding that, despite regulating hematopoietic development *in vitro*, double fusion-expression did not confer  
243 *in vivo* engraftment to hESC hematopoietic derivatives (Fig2D).

244

245 The increased hematopoietic output of double fusion-expressing hESCs might be the consequence of  
246 transgene-mediated proliferation/survival of the emerging HEPs or CD45+ cells. To address this, we  
247 analyzed cell cycle distribution (FigS2B) and apoptosis (FigS2C) within both HEPs and the CD45+ cell  
248 population. No differences in the proportion of either cycling HEPs or CD45+ cells were detected between

249 genotypes (25–36% for HEPs and 35–41% for CD45+ cells; **FigS2B**). Apoptotic levels were similarly low  
250 between the different genotypes of HEPs (6–8%) and CD45+ cells (5–7%) (**FigS2C**). Collectively, these  
251 results show that A4M cooperates with MA4 to induce HEP specification and blood commitment, without  
252 hijacking proliferation or survival of HEPs.

253

#### 254 **A4M and MA4 co-operate to enhance endothelial cell fate from HEPs**

255 We next addressed the developmental impact of A4M in endothelial maturation from HEPs<sup>10,47</sup>. We  
256 hypothesized that co-expression of A4M and MA4 in HEPs may (i) concomitantly promote subsequent  
257 endothelial and hematopoietic commitment or (ii) skew the hemato-endothelial commitment in favor of  
258 hematopoiesis. To test this, we analyzed the ability of HEPs to differentiate into mature endothelial cells.  
259 OP9-hESC co-cultures were dissociated on day 9 of development and HEPs were FACS-sorted and cultured  
260 for a week in endothelial-promoting conditions (**Fig4A**). The expression of the mature endothelial markers  
261 VE-cadherin (CD144), vWF, eNOS and CD31 was then analyzed. Irrespective of the genotype, HEPs  
262 cultured in endothelial conditions attached, became spindle-shaped, and formed VE-Cad+ endothelial-like  
263 structures co-expressing eNOS, vWF and CD31 (**Fig4B,C**, top panel). However, double fusion-expressing  
264 HEPs were more prone to differentiate into mature endothelial cells than single fusion-expressing HEPs.  
265 Accordingly, they yielded a 20-fold higher number of VE-Cad+ endothelial-like structures (**Fig4C**, top panel)  
266 and CD144+CD31+ endothelial cells (**Fig4C**, bottom panel). Interestingly, endothelial cells  
267 (HLA.ABC+CD31+CD34+CD144+CD45-CD43-) were found in the BM of mice transplanted with double fusion-  
268 expressing hESC blood derivatives at levels ~4-fold higher than in mice transplanted with single fusion-  
269 expressing cells (**Fig4D**).

270

271 Within CD34+CD31+CD45- HEPs, two subpopulations of phenotypically and functionally distinct HEPs can be  
272 distinguished based on the expression of CD34 and CD43: hemogenic HEPs (CD34<sup>low/+</sup>CD43+CD45-) and

273 endothelial HEPs (CD34<sup>++</sup>CD43<sup>-</sup>CD45<sup>-</sup>) (**Fig5A**)<sup>40,48,51</sup>. We thus analyzed the contribution of both HEP  
274 populations to the superior hematopoietic and endothelial differentiation observed in double fusion-  
275 expressing HEPs. Co-expression of A4M and MA4, but not single fusions, robustly enhanced the emergence  
276 of both endothelial and hemogenic HEPs (**Fig5B,C**). The identity of hemogenic and endothelial HEPs was  
277 confirmed by the specific expression of early hematopoietic and endothelial master genes (**Fig5D**). Thus,  
278 A4M cooperates with MA4 to promote hematopoietic and endothelial cell fate.

279

### 280 **Genome-wide transcriptomic and H3K79 methylation profiles support the developmental cooperation** 281 **between A4M and MA4**

282 To identify patterns of gene expression that might molecularly explain the functional co-operation between  
283 A4M and MA4 in hematopoietic specification, we performed RNA-seq analysis on FACS-purified EV-, MA4,  
284 A4M- and double fusion-expressing HEPs from day 15 hEBs. **Fig6A** shows a heatmap representation of the  
285 hierarchical clustering of the 335 genes differentially expressed between the four genotypes (**TableS2**).  
286 There is a clear transcriptomic transition towards a hematopoietic/endothelial gene signature from EV-HEPs  
287 to double-fusion-expressing HEPs. Single fusion-expressing HEPs clustered interspersed between EV and  
288 double-fusion HEPs. The biological functions affected by genes differentially expressed in MA4-, A4M- and  
289 double fusion-expressing HEPs relative to EV were classified by IPA software<sup>47,52</sup> and among the top  
290 significant enriched functional categories were “hematological system development and function”, “cancer”  
291 and “hematological disease” (**Fig6B**). Statistical (-log(p-value)) power shows distant effects of MA4 and A4M;  
292 however, co-expression of both fusions seems to establish a molecular balance/developmental cooperation  
293 in promoting blood-endothelial specification from hPSCs. Strikingly, biofunctions specifically associated to  
294 hematological lymphoid malignancies (not with non-hematological cancer) were predicted to be activated  
295 (positive z-score) exclusively in double fusion-expressing HEPs, further suggesting a molecular cooperation  
296 between MA4 and A4M in development and infant leukemia. (**Fig6C**).

297 The C-terminal-partners of MLL fusions normally interact with the histone methyltransferase DOT1L, which  
298 is the sole histone methyltransferase catalyzing histone 3 lysine 79 (H3K79) methylation, a chromatin  
299 modification widely associated with the dysregulated expression of *HOX-A* cluster genes in MLL leukemias  
300 <sup>13, 53</sup>. We thus performed genome-wide ChIP-seq analysis of the H3K79 trimethylation (H3K79me3) profiles  
301 in control, MA4-, A4M- and double fusion-expressing hESC-derived blood derivatives (**Fig7,S3A, TableS3**).  
302 In line with the RNA-seq data, functional analysis of the differential H3K79me3 peaks specific for double  
303 fusion-expressing cells revealed significant GO functional categories associated with "definitive  
304 hematopoiesis", "myeloid and erythroid differentiation/homeostasis" and "endothelial cell development"  
305 (**Fig7A,S3B**). This further supports the developmental co-operation between A4M and MA4 in promoting  
306 hemato-endothelial specification.

307

308 Finally, we analysed the H3K79me3 profiles at genomic loci of the classical MLL target genes reported by  
309 Guenther *et al*<sup>54</sup>. Non-*HOX-A* classical MLL targets such as *RUNX1*, *LMO2*, *ADMA10*, and *KDM6A* showed  
310 a slight although non-significant, enrichment of H3K79me3 in MA4-expressing hESCs, validating our ChIP-  
311 seq approach (**Fig7B**). However, enrichment of H3K79me3 in *HOX-A* cluster genes was observed  
312 exclusively in A4M-expressing cells although it was statistically significant only in double fusion-expressing  
313 differentiating hESCs (FDR<0.1) (**Fig7C**). **As such, *HOX-A* genes were up-regulated in double-fusion-  
314 expressing hematopoietic clonogenic progenitors (FigS3C)**. No differential enrichment of the repressive  
315 H3K4me2/3 mark was observed in either *HOX-A* or non-*HOX* genes in double fusion-expressing cells  
316 (**FigS4**). Collectively, these data suggest that the deregulated expression of *HOX-A* genes in MLL leukemias  
317 may be imposed by the reciprocal A4M fusion through a H3K79 methyltransferase activity. In support of this,  
318 a recent RNA-seq study performed in 42 infants with t(4;11)+ B-ALL enrolled in the Interfant treatment  
319 protocol, reveal that 45% of t(4;11)+ patients express the A4M fusion, and that *HOX-A* cluster genes are

320 exclusively expressed in this *AF4-MLL*-expressing subgroup of t(4;11)+ patients, who in fact display a  
321 significant more favorable clinical outcome<sup>19</sup>.

322

## 323 **DISCUSSION**

324

325 From an etiological and pathogenesis standpoint, infant cancer is distinct to adult cancer and should be  
326 studied as a developmental disease<sup>4,7,16</sup>. A biologically and clinically intriguing infant cancer is the t(4;11)+  
327 B-ALL, which is associated with a dismal outcome<sup>4,21,23</sup>. Evidence in support of its prenatal origin comes from  
328 studies in monozygotic twins and archived blood spots, providing compelling evidence of a single prenatal  
329 cell as the origin for t(4;11)<sup>5</sup>, and also from recent genome-wide studies demonstrating that this infant  
330 leukemia has one of the lowest frequencies of somatic mutations of any sequenced cancer<sup>55</sup>. The stable  
331 genome of these patients suggests that in infant developmental cancer, one “big-hit” might be sufficient for  
332 overt disease, supporting a key contribution of the prenatal cell-of-origin during a critical developmental  
333 window of stem cell vulnerability in leukemogenesis. However, despite its aggressiveness and short latency,  
334 our current understanding about its etiology, pathogenesis and cellular origin is still limited<sup>2,4,16,52</sup>. **Importantly,**  
335 **a recently developed xenograft model which represents the most *bona fide* model for t(4;11)+ B-ALL so far,**  
336 **has revealed the instructive role of MLL-Af4 in cord blood-derived CD34+ cells<sup>14</sup>.**

337

338 Studies using primary cells from t(4;11)+ B-ALL patients are incapable of addressing the developmental  
339 genesis of the hematopoietic system. **Recent data suggest that fetal liver lymphoid-primed multipotent**  
340 **progenitor may provide the developmental prerequisites for the initiation of t(4;11)+/MLL-AF4 infant**  
341 **leukemia<sup>56</sup>.** Because leukemogenesis manifests as a blockage or altered cell differentiation, the  
342 hematopoietic differentiation of hESCs may represent a promising *in vitro* model to study the onset of  
343 hematopoiesis and the earliest events leading to the specification of the hematopoietic cells<sup>36</sup>. Previous  
344 studies have addressed the oncogenic role of leukemic fusion genes in hESC-derived hematopoiesis<sup>57,58,59</sup>.

345 We previously explored the developmental impact of the pre-natal fusion MA4 in hESC hemato-endothelial  
346 development<sup>10</sup>, and found that MA4 expression promotes the emergence of endothelial-primed HEPs and  
347 further endothelial commitment, but hijacks the specification of hemogenic-primed HEPs, impairing  
348 hematopoietic output<sup>10</sup>.

349

350 The functional and molecular contribution of the reciprocal fusion genes resulting from the derivative  
351 translocated chromosomes remains obscure in cancer<sup>18,60</sup>. The MA4 fusion is always expressed in t(4;11)+B-  
352 ALL patients, whereas the reciprocal fusion A4M is expressed in only 45-50% of the patients<sup>18,60,19,20</sup>. Here,  
353 we took advantage of well-established hESC-based differentiation systems to study whether the A4M fusion  
354 cooperates with MA4 during early human hematopoietic and endothelial development. Co-expression of A4M  
355 and MA4 strongly promoted the emergence of HEPs, both endothelial-primed and hemogenic-primed.  
356 Moreover, the double fusion-expressing HEPs specified into significantly higher numbers of both  
357 hematopoietic and endothelial cells, irrespective of the *in vitro* differentiation protocol used and without  
358 affecting survival or proliferation, indicating a functional (developmental) co-operation between MA4 and A4M  
359 fusions during human hematopoietic development. This notion was confirmed by genome-wide  
360 transcriptomic analysis of differentiating HEPs. These developmental biology studies support previous  
361 evidence suggesting that A4M contributes to the pathobiology of t(4;11)+ B-ALL. Accordingly, Bursen<sup>11</sup>  
362 reported that A4M-transduced murine hematopoietic stem cells (HSCs) developed pro-B-ALL, whereas co-  
363 transduction with MA4 and A4M resulted in mixed lineage leukemia. Moreover, studies from Milne's  
364 laboratory demonstrated that RUNX1 is directly activated by MA4 and the RUNX1 protein interacts with the  
365 A4M protein, suggesting a mechanism of co-operation between the two fusion genes at the molecular level<sup>25</sup>.

366

367 In the embryo, definitive hematopoiesis cannot occur in the absence of endothelial cell development.  
368 Definitive HSCs in both mouse and human emerge from the hemogenic endothelium by a process known as

369 endothelial-to-hematopoietic transition<sup>61</sup>. Hematopoietic differentiation of hESCs occurs through the  
370 generation of HEPs, from which then originate both endothelial and hematopoietic cells. Here, co-expression  
371 of A4M and MA4 in HEPs concomitantly promoted endothelial and hematopoietic commitment rather than  
372 skewing the hemato-endothelial commitment in favor of one lineage over the other. This finding is important  
373 because beyond their pathogenic role in acute leukemias, the *MLL* gene is implicated in endothelial cell  
374 maturation, and endothelial dysfunction was recently linked to disease outcome in childhood leukemias<sup>31,32</sup>.  
375 Furthermore, other leukemia fusion oncogenes as well as lymphoma-specific genetic aberrations have been  
376 found in endothelial cells from chronic myeloid leukemia and B-cell lymphoma patients<sup>10,43,44</sup>, suggesting that  
377 endothelial cells may be part of the neoplastic clone. Also, BM-derived mesenchymal stem cells (BM-MSCs)  
378 from infant t(4;11)+ B-cell ALL were recently found to harbor and express the t(4;11) translocation<sup>33</sup>. The  
379 existence of a common embryonic precursor for MSCs and endothelial cells has been recently demonstrated  
380 by hESC-directed differentiation<sup>10,45</sup>. The finding of such a common embryonic precursor, and the presence  
381 of t(4;11) in both leukemic blasts and BM-MSCs of infant patients, suggests that the t(4;11) translocation  
382 arises and has a developmental impact on early pre-hematopoietic precursors. **As a technical caveat, it is**  
383 **important to emphasize that MA4 and A4M were sequentially transduced to allow for antibiotic selection and**  
384 **homogeneously-transduced hESC cultures. However, in double-fusion-expressing differentiating blood cells,**  
385 **MA4 was never individually expressed in the absence of A4M. When hematopoietic differentiation of hESCs**  
386 **was induced by EB formation both fusions were readily co-expressed, ruling out a biased functional**  
387 **phenotype driven by the sequential expression of each transgene in distinct developmental windows.**

388

389

390 Mechanistically, a putative function of A4M is to activate chromatin, rendering a chromatin landscape similar  
391 to that during stem cell development. It is currently unknown how A4M is able to reprogram chromatin, but it  
392 does contain the SET domain disrupted from its "specification domain", the N-terminal portion of MLL, which



393 binds to MEN1 and LEDGF, shaping the gene targeting module of the MLL gene. When A4M is expressed,  
394 the N-terminal portion is substituted by the AF4 N-terminus, which is the crucial domain (AF4N) that binds to  
395 and strongly activates RNA polymerase II (RNAP II) for transcriptional elongation. Overexpression of either  
396 AF4, AF4N or the fusion protein A4M induces robust RNAP II-dependent gene transcription by overwriting  
397 the elongation control process in a dominant fashion<sup>62-64</sup>. Since gene transcription *per se* and in particular  
398 “sterile” transcription is a powerful mechanism for chromatin activation, A4M could potentiate MA4 to skew  
399 normal and leukemic hematopoietic cell fate decisions. This also explains why MA4 has a more prominent  
400 role in the disease than the reciprocal A4M. If A4M functioned to initiate this process only by itself, then it  
401 would become obsolete after fulfilling the "chromatin opening job". However, transcription factors like MA4,  
402 RUNX1 or others then establish the transcriptional program leading to leukemogenesis. This is reflected in  
403 the enhanced hematopoietic potential of double fusion-expressing hESCs and the enriched H3K79me3  
404 activation mark in *HOX-A* cluster genes exclusively when MA4 and A4M are co-expressed. Thus, A4M  
405 prepares other transcription factors to become oncoproteins.

406

407 Molecularly, C-terminal-partners of MLL fusions (AF4, AF9, ENL) interact with DOT1L, which is the sole  
408 histone methyltransferase catalyzing H3K79 methylation, a chromatin modification widely associated with the  
409 dysregulated expression of *HOX-A* gene cluster in MLL-rearranged leukemias<sup>13,53</sup>. Here, ChIP-seq analysis  
410 of differentially enriched H3K79me3 genomic regions confirmed a hematopoietic/endothelial cell  
411 differentiation signature in double fusion-expressing HEPs, and revealed a significant enrichment of H3K79  
412 methylated regions specifically associated with *HOX-A* cluster MLL target genes (but not to non-*HOX-A* MLL  
413 targets) in double fusion-expressing differentiating hematopoietic cells. This is in line with the recently found  
414 significant positive correlation between the upregulation of the *HOX-A* gene cluster and the expression of  
415 A4M in primary t(4;11)+ infant B-cell ALL samples, and with previous studies identifying that approximately  
416 one-half of t(4;11)+ patients do not have an activated *HOX-A* signature<sup>20,65,66</sup>. This may explain why MA4

417 failed recently to bind to *HOX-A* genes to regulate *HOXA* gene expression<sup>14</sup>. Collectively, MA4 and A4M  
418 might cooperate through a complex molecular interaction to control *HOX-A* gene regulation<sup>25</sup>. In sum, we  
419 describe a functional and molecular cooperation between MA4 and A4M fusions during human hematopoietic  
420 development, and demonstrate how hESC-based hematopoietic differentiation represents a promising  
421 system to explore the developmental impact of the chimeric proteins resulting from chromosomal  
422 translocations, which remains obscure in human leukemia.

423 **AUTHOR CONTRIBUTION:** C.B. conceived the study, designed and performed experiments and analyzed  
424 data. P.M. conceived the study, designed experiments, analyzed data and wrote the manuscript. F.C.N.,  
425 X.W., R.V.M., F.G-A., H.R.H., V.A., P.J.R., D.A., L.E., R-T-R., A.A-D., J.dB. performed experiments and  
426 analyzed data. I.V., A.B., B.G., and R.M. contributed intellectually and financially.

427

428 **ACKNOWLEDGMENTS.** Financial support for this work was obtained from the European Research Council  
429 (CoG-2014-646903 and PoC-2018-811220) and the Generalitat de Catalunya (SGR330 and PERIS 2017-  
430 2019) to PM, the Spanish Ministry of Economy and Competitiveness (SAF2016-80481-R and SAF2016-  
431 76758-R) to PM and IV, the Spanish Association against cancer (AECC-CI-2015) to CB, the Health Institute  
432 Carlos III (ISCIII/FEDER, PI17/01028 and PI17/01028) to CB and PJR, the NIHR GOSH BRC and Great  
433 Ormond Street Hospital Children's Charity to J.dB, and Bloodwise and Cancer Research UK to BG. RM and  
434 PM were also supported by the Deutsche José Carreras Leukämie Stiftung. PM also acknowledges financial  
435 support from the Obra Social La Caixa-Fundació Josep Carreras. R-T-R is supported by a fellowship from  
436 the Spanish Association of Cancer Research (AECC). RV-M is supported by a Torres Quevedo fellowship  
437 by Spanish Ministry of Science and Innovation (PTQ-16-08623). P.M is an investigator of the Spanish Cell  
438 Therapy cooperative network (TERCEL).

439

440 **CONFLICT OF INTEREST DISCLOSURE:** The authors have nothing to disclose.

441

442

443

444

445

446

447 **REFERENCES**

448 1. Milne TA. Mouse models of MLL leukemia: recapitulating the human disease. *Blood*.  
449 2017;129(16):2217-23.

450

451 2. Montes R, Ayllon V, Prieto C, Bursen A, Prella C, Romero-Moya D, et al. Ligand-independent FLT3  
452 activation does not cooperate with MLL-AF4 to immortalize/transform cord blood CD34+ cells. *Leukemia*.  
453 2014;28(3):666-74.

454

455 3. Stam RW, den Boer ML, Schneider P, Nollau P, Horstmann M, Beverloo HB, et al. Targeting FLT3  
456 in primary MLL-gene-rearranged infant acute lymphoblastic leukemia. *Blood*. 2005;106(7):2484-90.

457

458 4. Sanjuan-Pla A, Bueno C, Prieto C, Acha P, Stam RW, Marschalek R, et al. Revisiting the biology of  
459 infant t(4;11)/MLL-AF4+ B-cell acute lymphoblastic leukemia. *Blood*. 2015;126(25):2676-85.

460

461 5. Ford AM, Ridge SA, Cabrera ME, Mahmoud H, Steel CM, Chan LC, et al. In utero rearrangements  
462 in the trithorax-related oncogene in infant leukaemias. *Nature*. 1993;363(6427):358-60.

463

464 6. Greaves M. Infection, immune responses and the aetiology of childhood leukaemia. *Nat Rev Cancer*.  
465 2006;6(3):193-203.

466

467 7. Bueno C, Montes R, Catalina P, Rodriguez R, Menendez P. Insights into the cellular origin and  
468 etiology of the infant pro-B acute lymphoblastic leukemia with MLL-AF4 rearrangement. *Leukemia*.  
469 2011;25(3):400-10.

470

471 8. Barrett NA, Malouf C, Kapeni C, Bacon WA, Giotopoulos G, Jacobsen SE, et al. MLL-AF4 Confers  
472 Enhanced Self-Renewal and Lymphoid Potential during a Restricted Window in Development. *Cell Rep*.  
473 2016;16(4):1039-54.

474

475 9. Bueno C, Ayllon V, Montes R, Navarro-Montero O, Ramos-Mejia V, Real PJ, et al. FLT3 activation  
476 cooperates with MLL-AF4 fusion protein to abrogate the hematopoietic specification of human ESCs. *Blood*.  
477 2013;121(19):3867-78, S1-3.

478

- 479 10. Bueno C, Montes R, Melen GJ, Ramos-Mejia V, Real PJ, Ayllon V, et al. A human ESC model for  
480 MLL-AF4 leukemic fusion gene reveals an impaired early hematopoietic-endothelial specification. *Cell Res.*  
481 2012;22(6):986-1002.  
482
- 483 11. Bursen A, Schwabe K, Ruster B, Henschler R, Ruthardt M, Dingermann T, et al. The AF4.MLL fusion  
484 protein is capable of inducing ALL in mice without requirement of MLL.AF4. *Blood.* 2010;115(17):3570-9.  
485
- 486 12. Chen W, Li Q, Hudson WA, Kumar A, Kirchhof N, Kersey JH. A murine Mll-AF4 knock-in model  
487 results in lymphoid and myeloid deregulation and hematologic malignancy. *Blood.* 2006;108(2):669-77.  
488
- 489 13. Krivtsov AV, Feng Z, Lemieux ME, Faber J, Vempati S, Sinha AU, et al. H3K79 methylation profiles  
490 define murine and human MLL-AF4 leukemias. *Cancer Cell.* 2008;14(5):355-68.  
491
- 492 14. Lin S, Luo RT, Ptasinska A, Kerry J, Assi SA, Wunderlich M, et al. Instructive Role of MLL-Fusion  
493 Proteins Revealed by a Model of t(4;11) Pro-B Acute Lymphoblastic Leukemia. *Cancer Cell.* 2016;30(5):737-  
494 49.  
495
- 496 15. Metzler M, Forster A, Pannell R, Arends MJ, Daser A, Lobato MN, et al. A conditional model of MLL-  
497 AF4 B-cell tumorigenesis using invertebrate technology. *Oncogene.* 2006;25(22):3093-103.  
498
- 499 16. Montes R, Ayllon V, Gutierrez-Aranda I, Prat I, Hernandez-Lamas MC, Ponce L, et al. Enforced  
500 expression of MLL-AF4 fusion in cord blood CD34+ cells enhances the hematopoietic repopulating cell  
501 function and clonogenic potential but is not sufficient to initiate leukemia. *Blood.* 2011;117(18):4746-58.  
502
- 503 17. Tamai H, Miyake K, Takatori M, Miyake N, Yamaguchi H, Dan K, et al. Activated K-Ras protein  
504 accelerates human MLL/AF4-induced leukemo-lymphomogenicity in a transgenic mouse model. *Leukemia.*  
505 2011;25(5):888-91.  
506
- 507 18. Kowarz E, Burmeister T, Lo Nigro L, Jansen MW, Delabesse E, Klingebiel T, et al. Complex MLL  
508 rearrangements in t(4;11) leukemia patients with absent AF4.MLL fusion allele. *Leukemia.* 2007;21(6):1232-  
509 8.  
510
- 511 19. Agraz-Doblas A, Bueno C., Bashford-Rogers R., Anindita R., Schneider P., Bardini M., Ballerini P.,  
512 Cazzaniga G., Moreno T., Revilla C., Gut M., De Lorenzo P., Valsecchi MG, Roberts I, Pieters R, Varela I.,  
513 Menendez P., Stam R.W. Unravelling the cellular origin and clinical prognosis markers of infant B-cell acute  
514 lymphoblastic leukemia using genome-wide analysis. *Haematologica.* 2019;in press.  
515
- 516 20. Trentin L, Giordan M, Dingermann T, Basso G, Te Kronnie G, Marschalek R. Two independent gene  
517 signatures in pediatric t(4;11) acute lymphoblastic leukemia patients. *Eur J Haematol.* 2009;83(5):406-19.  
518
- 519 21. Kumar AR, Yao Q, Li Q, Sam TA, Kersey JH. t(4;11) leukemias display addiction to MLL-AF4 but not  
520 to AF4-MLL. *Leuk Res.* 2011;35(3):305-9.  
521
- 522 22. Sanders DS, Muntean AG, Hess JL. Significance of AF4-MLL reciprocal fusion in t(4;11) leukemias?  
523 *Leuk Res.* 2011;35(3):299-300.  
524

- 525 23. Prieto C, Marschalek R, Kuhn A, Bursen A, Bueno C, Menendez P. The AF4-MLL fusion transiently  
526 augments multilineage hematopoietic engraftment but is not sufficient to initiate leukemia in cord blood  
527 CD34(+) cells. *Oncotarget*. 2017;8(47):81936-41.  
528
- 529 24. Rego EM, Pandolfi PP. Reciprocal products of chromosomal translocations in human cancer  
530 pathogenesis: key players or innocent bystanders? *Trends Mol Med*. 2002;8(8):396-405.  
531
- 532 25. Wilkinson AC, Ballabio E, Geng H, North P, Tapia M, Kerry J, et al. RUNX1 is a key target in t(4;11)  
533 leukemias that contributes to gene activation through an AF4-MLL complex interaction. *Cell Rep*.  
534 2013;3(1):116-27.  
535
- 536 26. Menendez P, Bueno C, Wang L. Human embryonic stem cells: A journey beyond cell replacement  
537 therapies. *Cytotherapy*. 2006;8(6):530-41.  
538
- 539 27. Romero-Moya D, Santos-Ocana C, Castano J, Garrabou G, Rodriguez-Gomez JA, Ruiz-Bonilla V,  
540 et al. Genetic Rescue of Mitochondrial and Skeletal Muscle Impairment in an Induced Pluripotent Stem Cells  
541 Model of Coenzyme Q10 Deficiency. *Stem Cells*. 2017;35(7):1687-703.  
542
- 543 28. Menendez P, Vargas A, Bueno C, Barrera S, Almeida J, De Santiago M, et al. Quantitative analysis  
544 of bcl-2 expression in normal and leukemic human B-cell differentiation. *Leukemia*. 2004;18(3):491-8.  
545
- 546 29. Ramos-Mejia V, Melen GJ, Sanchez L, Gutierrez-Aranda I, Ligerio G, Cortes JL, et al. Nodal/Activin  
547 signaling predicts human pluripotent stem cell lines prone to differentiate toward the hematopoietic lineage.  
548 *Mol Ther*. 2010;18(12):2173-81.  
549
- 550 30. Wang L, Li L, Shojaei F, Levac K, Cerdan C, Menendez P, et al. Endothelial and hematopoietic cell  
551 fate of human embryonic stem cells originates from primitive endothelium with hemangioblastic properties.  
552 *Immunity*. 2004;21(1):31-41.  
553
- 554 31. Diehl F, Rossig L, Zeiher AM, Dimmeler S, Urbich C. The histone methyltransferase MLL is an  
555 upstream regulator of endothelial-cell sprout formation. *Blood*. 2007;109(4):1472-8.  
556
- 557 32. Hatzipantelis ES, Athanassiou-Metaxa M, Gombakis N, Tzimouli V, Taparkou A, Sidi-Fragandrea V,  
558 et al. Thrombomodulin and von Willebrand factor: relation to endothelial dysfunction and disease outcome in  
559 children with acute lymphoblastic leukemia. *Acta Haematol*. 2011;125(3):130-5.  
560
- 561 33. Menendez P, Catalina P, Rodriguez R, Melen GJ, Bueno C, Arriero M, et al. Bone marrow  
562 mesenchymal stem cells from infants with MLL-AF4+ acute leukemia harbor and express the MLL-AF4 fusion  
563 gene. *J Exp Med*. 2009;206(13):3131-41.  
564
- 565 34. Ramos-Mejia V, Fernandez AF, Ayllon V, Real PJ, Bueno C, Anderson P, et al. Maintenance of  
566 human embryonic stem cells in mesenchymal stem cell-conditioned media augments hematopoietic  
567 specification. *Stem Cells Dev*. 2012;21(9):1549-58.  
568
- 569 35. Sanchez L, Gutierrez-Aranda I, Ligerio G, Martin M, Ayllon V, Real PJ, et al. Maintenance of human  
570 embryonic stem cells in media conditioned by human mesenchymal stem cells obviates the requirement of  
571 exogenous basic fibroblast growth factor supplementation. *Tissue Eng Part C Methods*. 2012;18(5):387-96.

- 572  
573 36. Bueno C, Montes R, Martin L, Prat I, Hernandez MC, Orfao A, et al. NG2 antigen is expressed in  
574 CD34+ HPCs and plasmacytoid dendritic cell precursors: is NG2 expression in leukemia dependent on the  
575 target cell where leukemogenesis is triggered? *Leukemia*. 2008;22(8):1475-8.  
576  
577 37. Castano J, Menendez P, Bruzos-Cidon C, Straccia M, Sousa A, Zabaleta L, et al. Fast and efficient  
578 neural conversion of human hematopoietic cells. *Stem Cell Reports*. 2014;3(6):1118-31.  
579  
580 38. Munoz-Lopez A, Romero-Moya D, Prieto C, Ramos-Mejia V, Agraz-Doblas A, Varela I, et al.  
581 Development Refractoriness of MLL-Rearranged Human B Cell Acute Leukemias to Reprogramming into  
582 Pluripotency. *Stem Cell Reports*. 2016;7(4):602-18.  
583  
584 39. Bueno C, Sardina JL, Di Stefano B, Romero-Moya D, Munoz-Lopez A, Ariza L, et al. Reprogramming  
585 human B cells into induced pluripotent stem cells and its enhancement by C/EBPalpha. *Leukemia*.  
586 2016;30(3):674-82.  
587  
588 40. Giorgetti A, Castano J, Bueno C, Diaz de la Guardia R, Delgado M, Bigas A, et al. Proinflammatory  
589 signals are insufficient to drive definitive hematopoietic specification of human HSCs in vitro. *Exp Hematol*.  
590 2017;45:85-93 e2.  
591  
592 41. Menendez P, Wang L, Chadwick K, Li L, Bhatia M. Retroviral transduction of hematopoietic cells  
593 differentiated from human embryonic stem cell-derived CD45(neg)PFV hemogenic precursors. *Mol Ther*.  
594 2004;10(6):1109-20.  
595  
596 42. Bueno C, Roldan M, Anguita E, Romero-Moya D, Martin-Antonio B, Rosu-Myles M, et al. Bone  
597 marrow mesenchymal stem cells from patients with aplastic anemia maintain functional and immune  
598 properties and do not contribute to the pathogenesis of the disease. *Haematologica*. 2014;99(7):1168-75.  
599  
600 43. Ramos-Mejia V, Navarro-Montero O, Ayllon V, Bueno C, Romero T, Real PJ, et al. HOXA9 promotes  
601 hematopoietic commitment of human embryonic stem cells. *Blood*. 2014;124(20):3065-75.  
602  
603 44. Toscano MG, Navarro-Montero O, Ayllon V, Ramos-Mejia V, Guerrero-Carreño X, Bueno C, et al.  
604 SCL/TAL1-mediated transcriptional network enhances megakaryocytic specification of human embryonic  
605 stem cells. *Mol Ther*. 2015;23(1):158-70.  
606  
607 45. Bueno C, Montes R, Menendez P. The ROCK inhibitor Y-27632 negatively affects the  
608 expansion/survival of both fresh and cryopreserved cord blood-derived CD34+ hematopoietic progenitor  
609 cells: Y-27632 negatively affects the expansion/survival of CD34+HSPCs. *Stem Cell Rev*. 2010;6(2):215-23.  
610  
611 46. Rubio R, Garcia-Castro J, Gutierrez-Aranda I, Paramio J, Santos M, Catalina P, et al. Deficiency in  
612 p53 but not retinoblastoma induces the transformation of mesenchymal stem cells in vitro and initiates  
613 leiomyosarcoma in vivo. *Cancer Res*. 2010;70(10):4185-94.  
614  
615 47. Ayllon V, Bueno C, Ramos-Mejia V, Navarro-Montero O, Prieto C, Real PJ, et al. The Notch ligand  
616 DLL4 specifically marks human hematoendothelial progenitors and regulates their hematopoietic fate.  
617 *Leukemia*. 2015;29(8):1741-53.  
618

- 619 48. Vodyanik MA, Slukvin, II. Hematoendothelial differentiation of human embryonic stem cells. *Curr*  
620 *Protoc Cell Biol.* 2007;Chapter 23:Unit 23 6.  
621
- 622 49. Bueno C, Montes R, de la Cueva T, Gutierrez-Aranda I, Menendez P. Intra-bone marrow  
623 transplantation of human CD34(+) cells into NOD/LtSz-scid IL-2rgamma(null) mice permits multilineage  
624 engraftment without previous irradiation. *Cytotherapy.* 2010;12(1):45-9.  
625
- 626 50. Gutierrez-Aranda I, Ramos-Mejia V, Bueno C, Munoz-Lopez M, Real PJ, Macia A, et al. Human  
627 induced pluripotent stem cells develop teratoma more efficiently and faster than human embryonic stem cells  
628 regardless the site of injection. *Stem Cells.* 2010;28(9):1568-70.  
629
- 630 51. Vodyanik MA, Bork JA, Thomson JA, Slukvin, II. Human embryonic stem cell-derived CD34+ cells:  
631 efficient production in the coculture with OP9 stromal cells and analysis of lymphohematopoietic potential.  
632 *Blood.* 2005;105(2):617-26.  
633
- 634 52. Prieto C, Stam RW, Agraz-Doblas A, Ballerini P, Camos M, Castano J, et al. Activated KRAS  
635 Cooperates with MLL-AF4 to Promote Extramedullary Engraftment and Migration of Cord Blood CD34+  
636 HSPC But Is Insufficient to Initiate Leukemia. *Cancer Res.* 2016;76(8):2478-89.  
637
- 638 53. Deshpande AJ, Deshpande A, Sinha AU, Chen L, Chang J, Cihan A, et al. AF10 regulates  
639 progressive H3K79 methylation and HOX gene expression in diverse AML subtypes. *Cancer Cell.*  
640 2014;26(6):896-908.  
641
- 642 54. Guenther MG, Lawton LN, Rozovskaia T, Frampton GM, Levine SS, Volkert TL, et al. Aberrant  
643 chromatin at genes encoding stem cell regulators in human mixed-lineage leukemia. *Genes Dev.*  
644 2008;22(24):3403-8.  
645
- 646 55. Andersson AK, Ma J, Wang J, Chen X, Gedman AL, Dang J, et al. The landscape of somatic  
647 mutations in infant MLL-rearranged acute lymphoblastic leukemias. *Nat Genet.* 2015;47(4):330-7.  
648
- 649 56. Malouf C, Ottersbach K. The fetal liver lymphoid-primed multipotent progenitor provides the  
650 prerequisites for the initiation of t(4;11) MLL-AF4 infant leukemia. *Haematologica.* 2018.  
651
- 652 57. Peters DG, Klucher KM, Perlingeiro RC, Dessain SK, Koh EY, Daley GQ. Autocrine and paracrine  
653 effects of an ES-cell derived, BCR/ABL-transformed hematopoietic cell line that induces leukemia in mice.  
654 *Oncogene.* 2001;20(21):2636-46.  
655
- 656 58. Ji J, Risueno RM, Hong S, Allan D, Rosten P, Humphries K, et al. Brief report: ectopic expression of  
657 NUP98-HOXA10 augments erythroid differentiation of human embryonic stem cells. *Stem Cells.*  
658 2011;29(4):736-41.  
659
- 660 59. Tan YT, Ye L, Xie F, Beyer AI, Muench MO, Wang J, et al. Respecifying human iPSC-derived blood  
661 cells into highly engraftable hematopoietic stem and progenitor cells with a single factor. *Proc Natl Acad Sci*  
662 *U S A.* 2018;115(9):2180-5.  
663
- 664 60. Marschalek R. Mechanisms of leukemogenesis by MLL fusion proteins. *Br J Haematol.*  
665 2011;152(2):141-54.

- 666  
667 61. Boisset JC, van Cappellen W, Andrieu-Soler C, Galjart N, Dzierzak E, Robin C. In vivo imaging of  
668 haematopoietic cells emerging from the mouse aortic endothelium. *Nature*. 2010;464(7285):116-20.  
669  
670 62. Ahmad K, Scholz B, Capelo R, Schweighofer I, Kahnt AS, Marschalek R, et al. AF4 and AF4-MLL  
671 mediate transcriptional elongation of 5-lipoxygenase mRNA by 1, 25-dihydroxyvitamin D3. *Oncotarget*.  
672 2015;6(28):25784-800.  
673  
674 63. Benedikt A, Baltruschat S, Scholz B, Bursen A, Arrey TN, Meyer B, et al. The leukemogenic AF4-  
675 MLL fusion protein causes P-TEFb kinase activation and altered epigenetic signatures. *Leukemia*.  
676 2011;25(1):135-44.  
677  
678 64. Muck F, Bracharz S, Marschalek R. DDX6 transfers P-TEFb kinase to the AF4/AF4N (AFF1) super  
679 elongation complex. *Am J Blood Res*. 2016;6(3):28-45.  
680  
681 65. Driessen EM, van Roon EH, Spijkers-Hagelstein JA, Schneider P, de Lorenzo P, Valsecchi MG, et  
682 al. Frequencies and prognostic impact of RAS mutations in MLL-rearranged acute lymphoblastic leukemia in  
683 infants. *Haematologica*. 2013;98(6):937-44.  
684  
685 66. Kuhn A, Loscher D, Marschalek R. The IRX1/HOXA connection: insights into a novel t(4;11)- specific  
686 cancer mechanism. *Oncotarget*. 2016;7(23):35341-52.  
687  
688  
689



690 **FIGURE LEGENDS**

691 **Figure 1. Characterization of transgenic human ESCs expressing the reciprocal fusion A4M together**  
692 **with MA4. (A)** RNA-seq and qRT-PCR validation revealed that ~45% (11/25) of the patients with t(4;11)+ B-  
693 ALL do not express the reciprocal fusion A4M<sup>18</sup>. **(B)** *Left*, Phase-contrast morphology of representative  
694 colonies from each transgenic hESC line. *Right*, RT-PCR confirming expression of both fusions in  
695 undifferentiated hESCs. **(C)** qRT-PCR expression of the pluripotency genes *OCT4*, *SOX2*, *NANOG*,  
696 *CRIPTO*, and *DNMT3B*. **(D)** Representative FACS data confirming expression of the pluripotency surface  
697 makers SSEA-3, SSEA-4, TRA-1-60, and TRA-1-81.

698

699 **Figure 2. A4M cooperates with MA4 to accelerate human ESC/EB specification towards HEPs and**  
700 **subsequent hematopoietic differentiation. (A)** Schematic of EB hematopoietic differentiation of hESCs  
701 and end-point analyses. **(B)** *Upper left*, specification into HEPs (CD31<sup>+</sup>CD34<sup>+</sup>CD45<sup>-</sup>) is accelerated in double  
702 fusion-expressing hESCs. Subsequent differentiation of HEPs into hematopoietic progenitors (*upper right*)  
703 and mature CD45<sup>+</sup> blood cells (*bottom left*) is enhanced in double fusion-expressing HEPs. *Bottom right*, CFU  
704 read-out and scoring (pie charts) confirming an accelerated and enhanced hematopoietic progenitor potential  
705 from double fusion-expressing blood derivatives. **(C)** RT-PCR confirming stable expression of MA4 and A4M  
706 upon EB differentiation. **(D)** Neither MA4- nor double fusion-expressing blood derivatives display *in vivo*  
707 hematopoietic engraftment potential in irradiated NSG mice. Data are presented as mean±SEM from at least  
708 three independent experiments. \*p<0.05.

709

710 **Figure 3. Co-expression of MA4 and A4M enhances hematopoietic differentiation of human ESCs in**  
711 **OP9 co-culture. (A)** Experimental design of OP9-based hESC differentiation towards HEPs and further  
712 hematopoietic commitment of HEPs maintained in either liquid culture for 16 days or in MS5 co-culture for  
713 30 days. **(B)** Frequency of total CD45<sup>+</sup> blood cells after 9 days in OP9 co-culture. **(C,D)** CD45<sup>-</sup>CD31<sup>+</sup>CD34<sup>+</sup>

714 HEPs were FACS-purified at day 9 of OP9 co-culture and allowed to differentiate into CD45<sup>+</sup> cells in liquid  
715 culture (C) or in MS5 co-culture (D). Data represent mean±SEM from independent experiments.

716

717 **Figure 4. Enhanced endothelial cell fate from HEPs co-expressing MA4 and A4M.** (A) Scheme of HEPs  
718 endothelial differentiation and phenotypic characterization. (B) FACS-sorted HEPs from day 9 human ESC-  
719 OP9 co-cultures were cultured in EGM2 medium for 5 days and analyzed by immunofluorescence for VE-  
720 cadherin, eNOS and vWF. (C) *Top*, Endothelial-like structures were identified and quantified based on VE-  
721 cadherin staining (white dotted-lined areas in B, *top panel*). *Bottom*, Frequency of CD45<sup>+</sup>CD31<sup>+</sup>CD144<sup>+</sup>  
722 endothelial cells quantified by flow cytometry. (D) *In vivo* endothelial engraftment potential  
723 (HLA.ABC<sup>+</sup>CD31<sup>+</sup>CD144<sup>+</sup>CD45<sup>-</sup>) analyzed in bone marrow of NSG mice 8 weeks after transplantation of  
724 HEPs. Data presented as mean±SEM from 5 independent experiments. \*p<0.05.

725

726 **Figure 5. Co-expression of MA4 and A4M significantly enhances the emergence of both endothelial**  
727 **and hemogenic HEPs.** (A) Representative flow cytometry analysis of HEPs with hemogenic (CD45-  
728 CD31<sup>+</sup>CD43<sup>+</sup>CD34<sup>dim/+</sup>) and endothelial (CD45<sup>-</sup>CD31<sup>+</sup>CD43<sup>-</sup>CD34<sup>++</sup>) potential. (B,C) A4M cooperates with  
729 MA4 to boost the emergence of both endothelial (B) and hemogenic (C) HEPs. Data presented as  
730 mean±SEM from 3 independent experiments. (D) Expression of *RUNX1c* and *Ve-Cad* in hemogenic and  
731 endothelial HEPs. \* p<0.05

732

733 **Figure 6: Transcriptional transition towards a hematopoietic/endothelial gene signature in double**  
734 **fusion-expressing HEPs.** (A) Heatmap representation of hierarchical clustering of genes differentially  
735 expressed between EV-, single fusions- and double fusion-expressing HEPs. Each column represents a  
736 technical replicate from three independent experiments. (B,C) Statistically significant functional categories  
737 (B) and cancer/leukemia-associated biofunctions (C) identified using IPA on genes differentially expressed

738 in single fusions-, and double fusion-expressing HEPs relative to EV. They are ranked by z-score. Functional  
739 categories associated with “hematological system development and function” and “cardiovascular system  
740 development” are shown in bold. All significant biofunctions are associated with blood cell differentiation,  
741 homeostasis and migration/movement.

742

743 **Figure 7: H3K79 methylation profiles at genomic loci of MLL targets in MA4-, A4M- and double fusion-**  
744 **expressing human ESC-derived blood derivatives. (A)** GO enrichment of differential H3K79me3 peaks  
745 specific for double fusion-expressing cells. **(B-C)** Representative profiles for ChIP-seq using anti-H3K79me<sup>3</sup>  
746 antibody at genomic regions of typical non-HOXA **(B)** and *HOXA* MLL targets **(C)**.

747

748

749

750

751

752

753

754

755

756

757

758

759

760

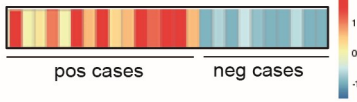
761

**A**

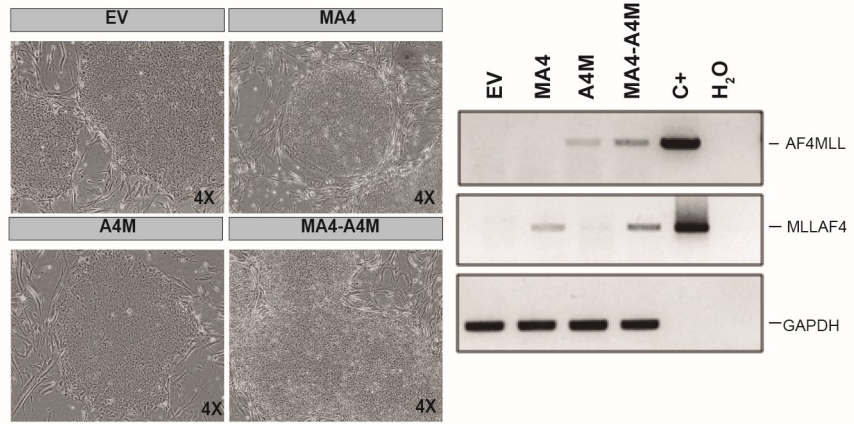
Infant BCP-ALL  
t(4;11)/MA4<sup>+</sup>



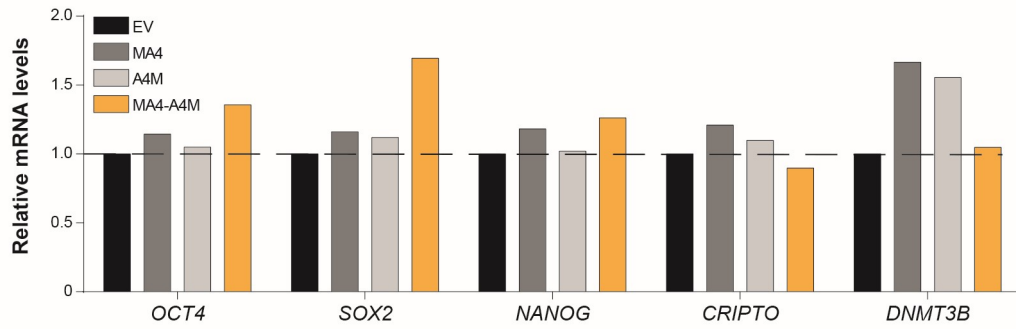
RNA-Seq A4M expression



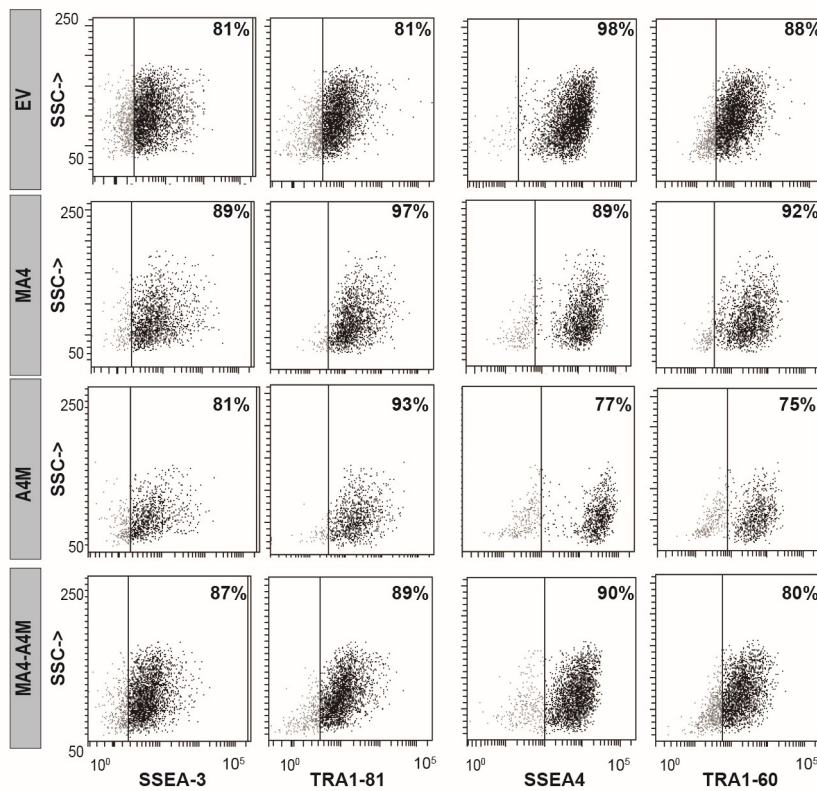
**B**



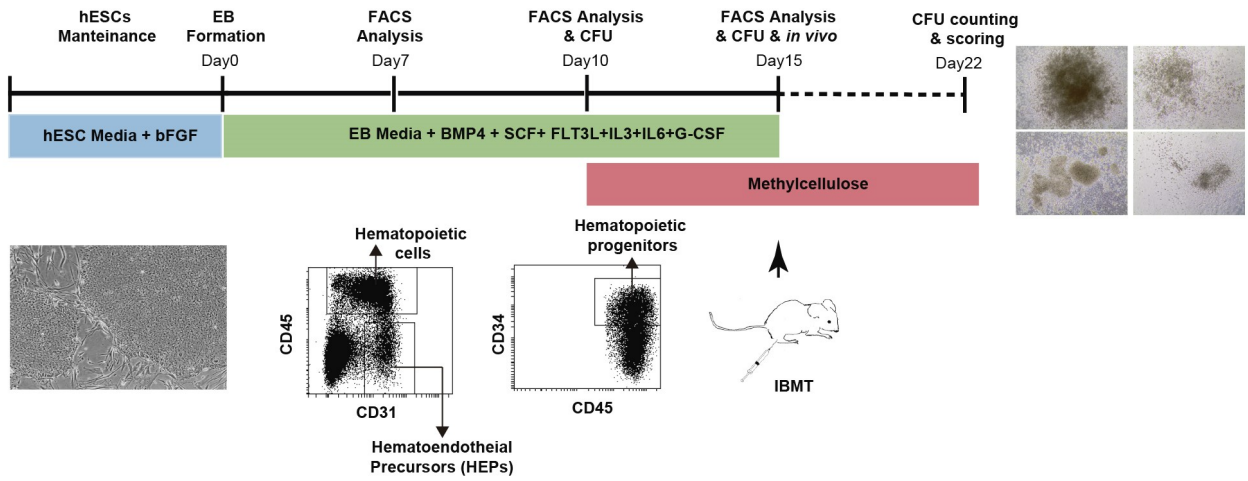
**C**



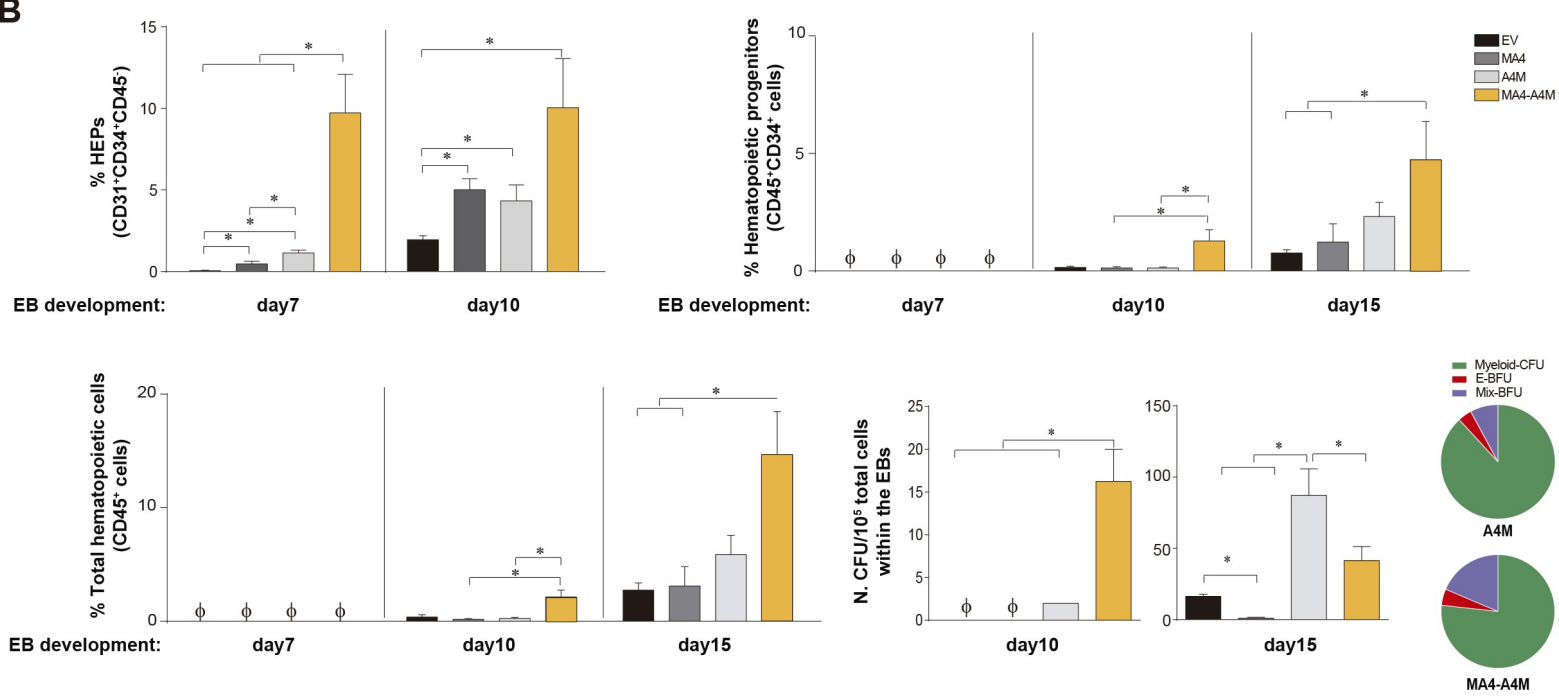
**D**



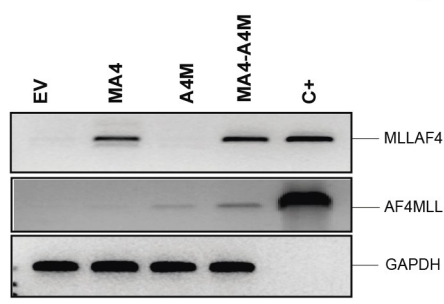
A



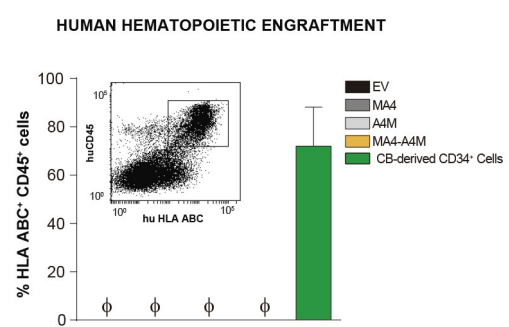
B



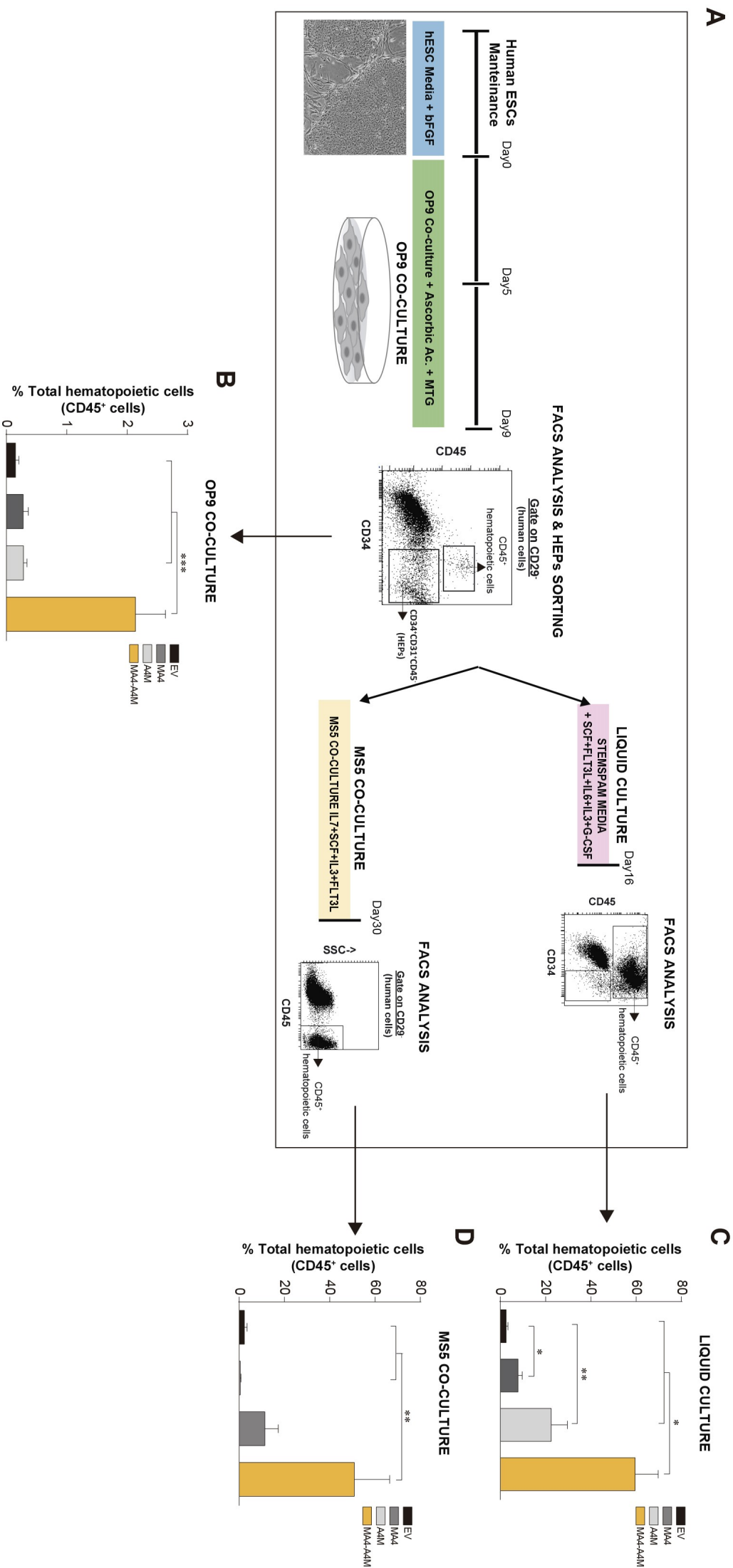
C



D



Bueno C *et al.* Figure 3



**A**

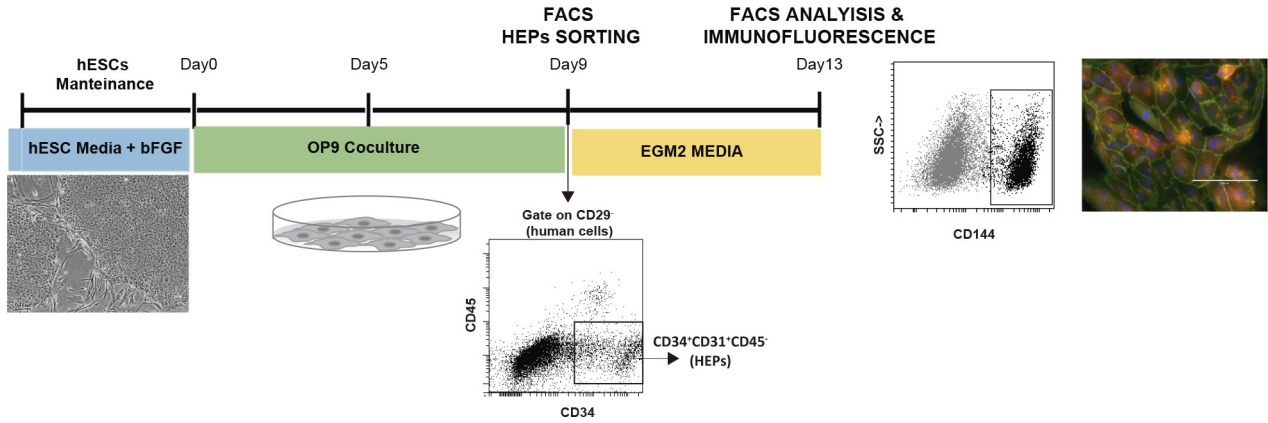
**B**

**C**

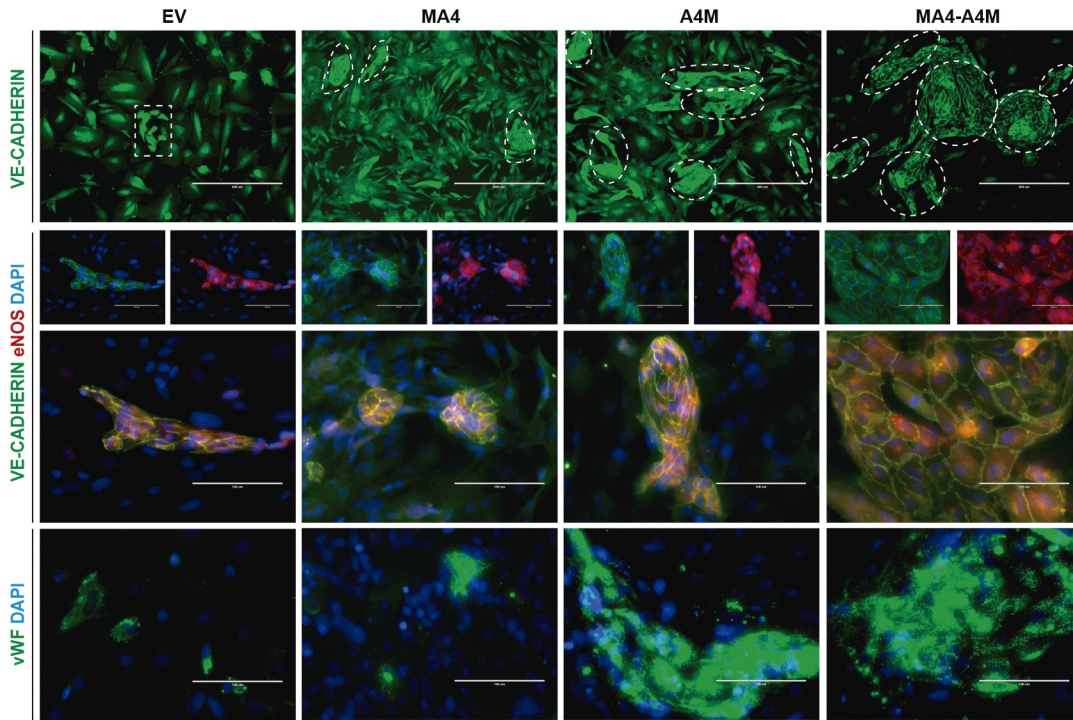
**D**



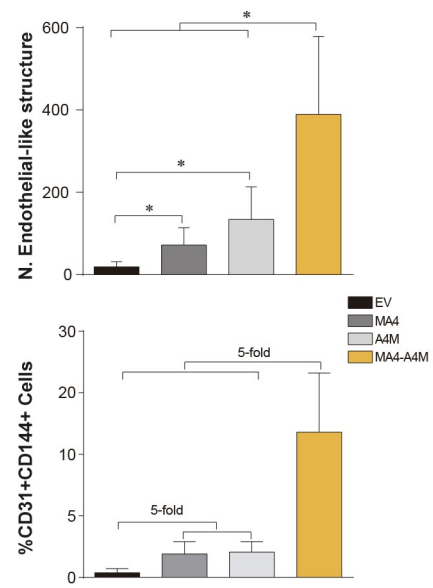
**A**



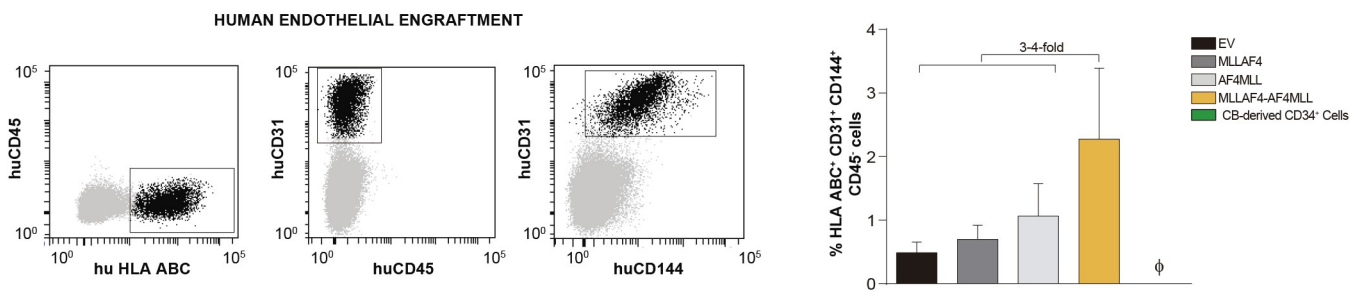
**B**

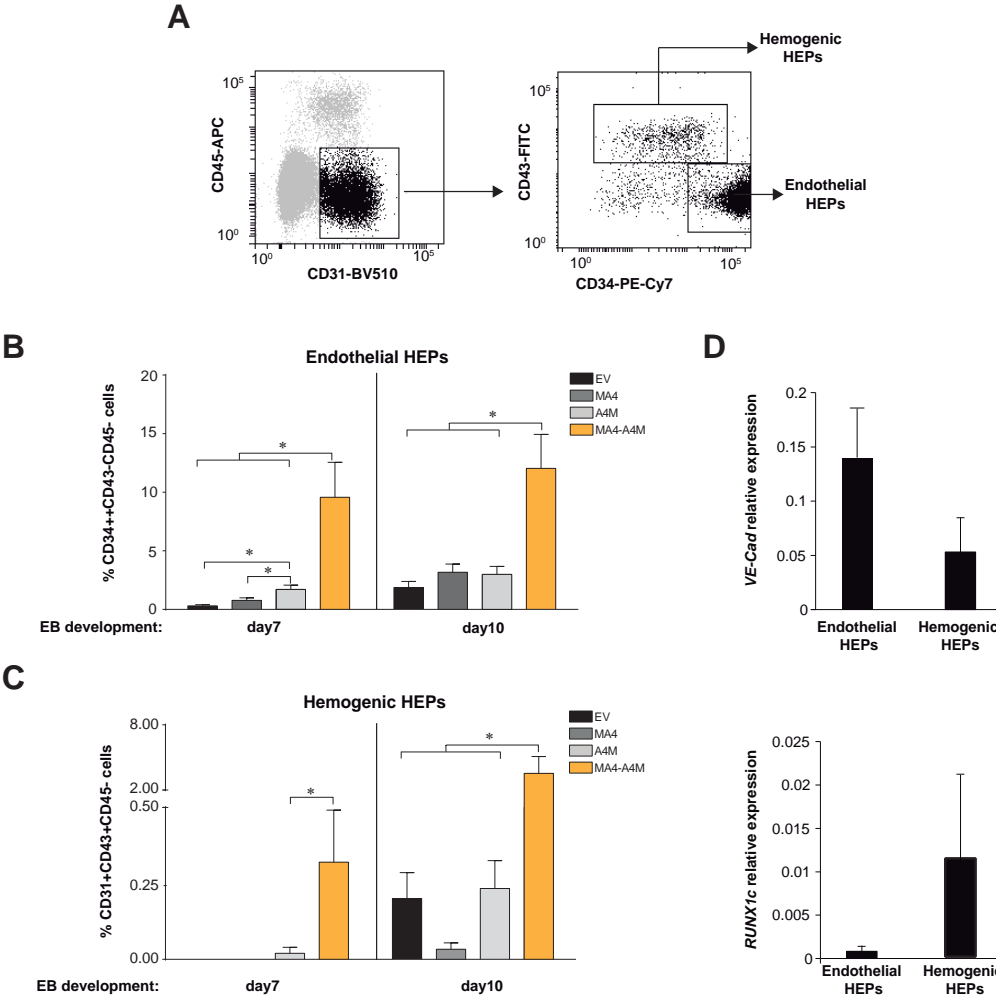


**C**



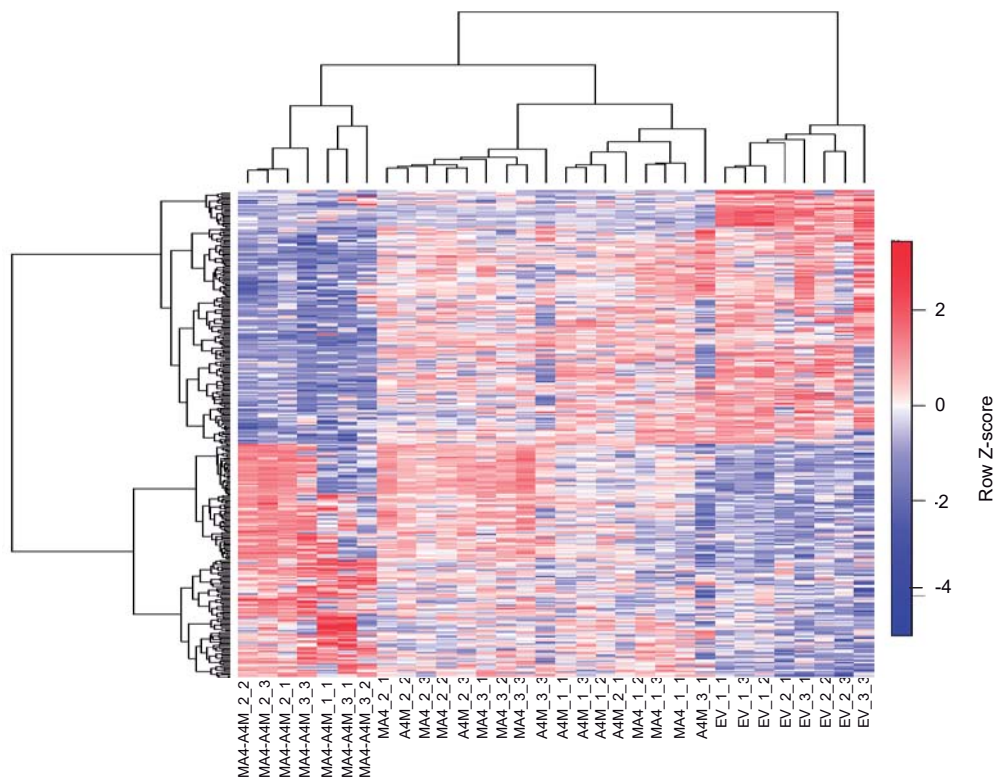
**D**



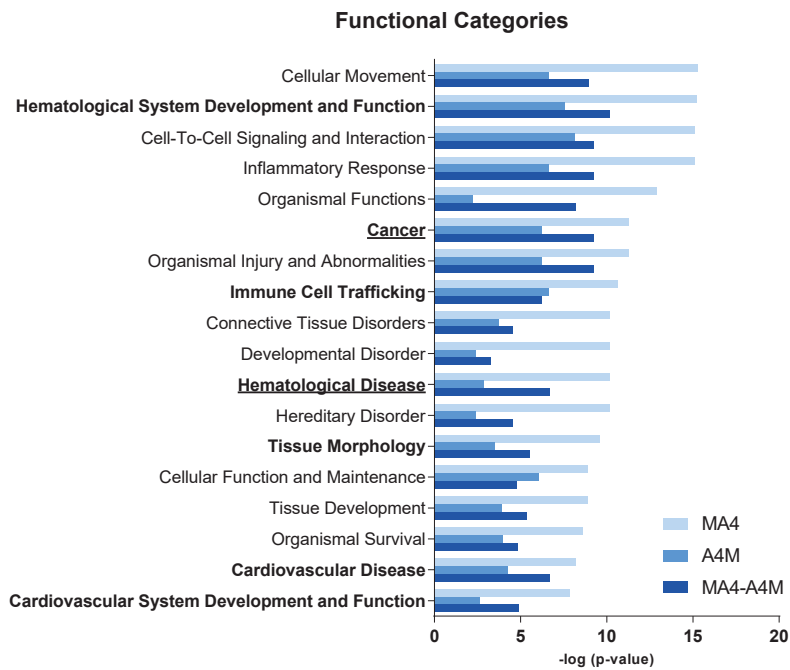




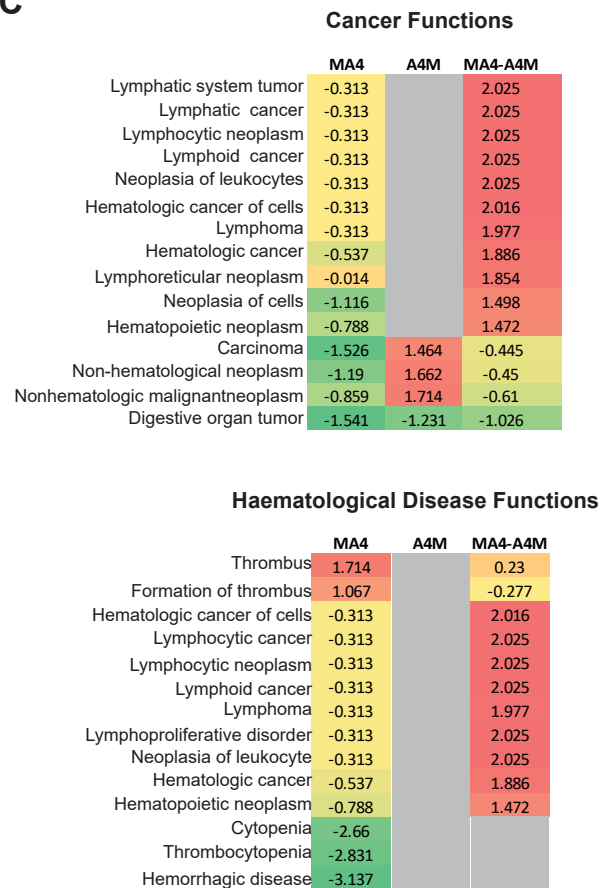
A



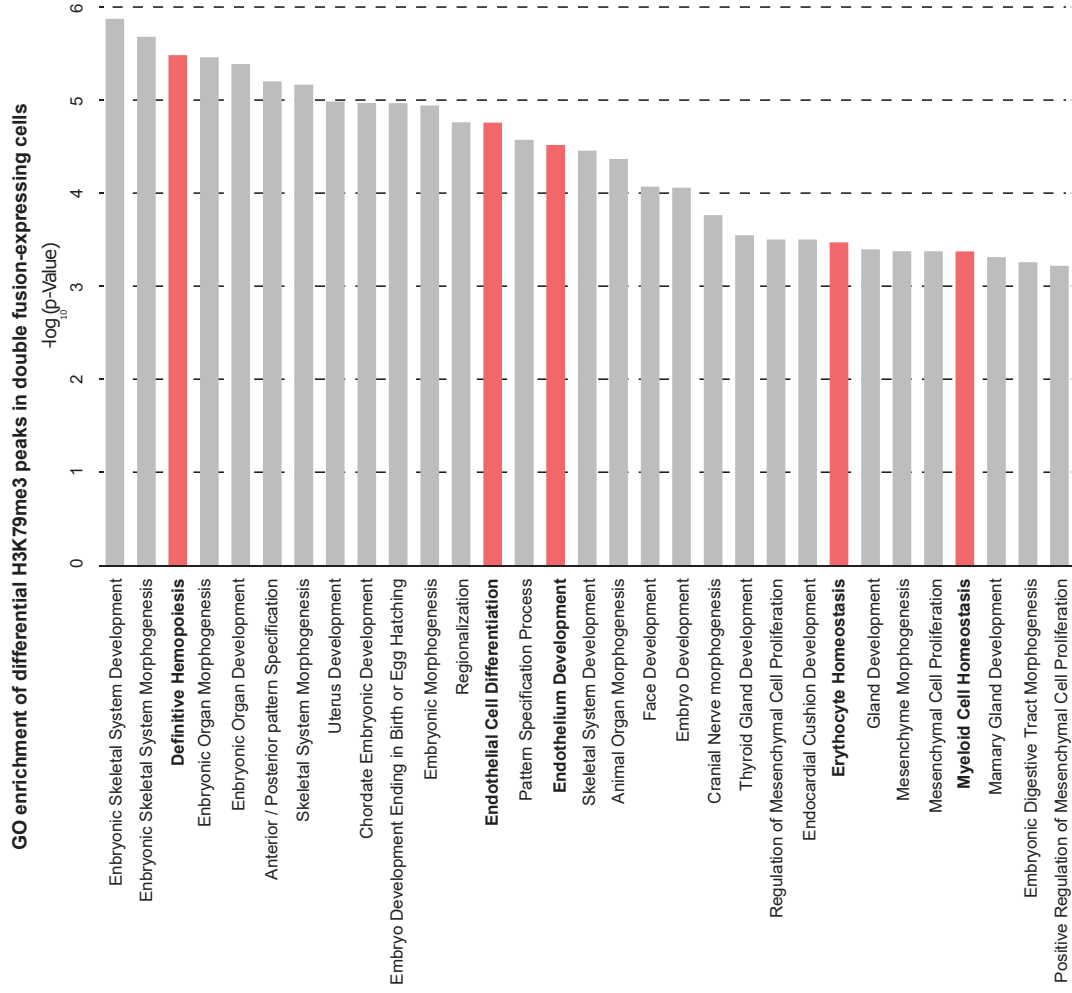
B



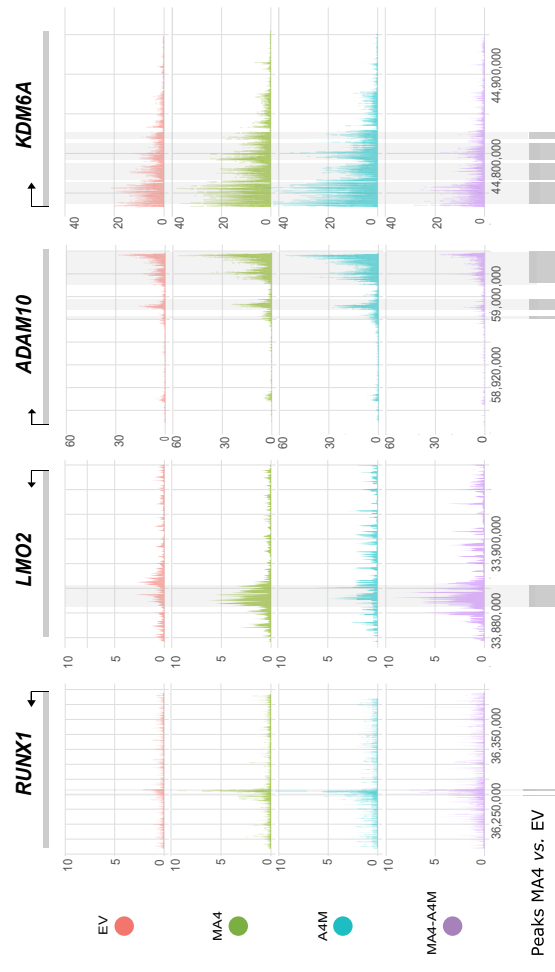
C



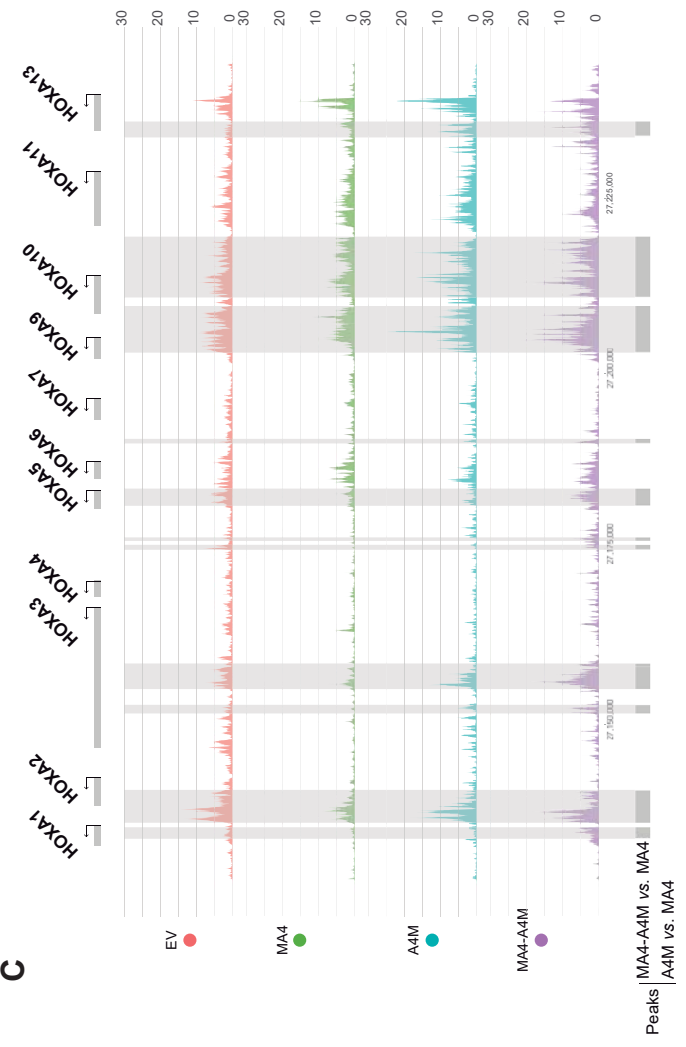
A



B



C



## **SUPPLEMENTARY LEGENDS AND METHODS**

### **Chromatin immunoprecipitation Sequencing**

One million day 15 hematopoietic differentiating hEB-derived cells were subjected to Chromatin Immunoprecipitation (ChIP) as described<sup>1</sup>. Briefly, formaldehyde crosslinked cell extracts were sonicated using a Bioruptor (Diagenode) with a 0.5-min interval protocol to obtain DNA fragments of 200–500 bp. The chromatin fraction was divided into three parts and incubated overnight with 2 µg of anti-H3K4me3, anti-H3K79me3, or anti-H3 antibodies (Abcam) in RIPA buffer, and precipitated with protein A/G-Sepharose (Amersham). Cross-linkage of the co-precipitated DNA-protein complexes was reversed, and the DNA was sequenced at the CRG-CNAG Genomics Facility. Paired-end 50 bp ChIP-seq data reads were generated using a HiSeq 2500 Illumina sequencer. Alignment and peak detection was performed using the ENCODE (phase-3) histone ChIP-seq pipeline specifications. Reads were aligned to the human reference genome (assembly hg19) using BWA<sup>2</sup>, removing all reads with a quality score <30. Peaks were called using MACS2<sup>3</sup> and whole cell extract samples as background samples. Differential analysis of histone mark peaks between experimental groups and the EV control group was performed using DiffBind<sup>4</sup>, with a False Discovery Rate (FDR) cut-off of 0.1. Peaks annotation and Gene Ontology (GO) enrichment were analyzed with ChIP-Enrich package in R<sup>4</sup>, using an FDR threshold of 0.1. ChIP-Seq data is deposited and available at Gene Expression Omnibus (GEO, accession number GSE111263).

### **Low-input RNA-seq and bulk RNA-seq on t(4;11)+B-ALL patients**

For low-input RNAseq, 50 HEPs were FACS-purified from day 15 EBs into individual wells of a 96-well PCR plate containing lysis buffer (0.2% Triton-X100 and 2.3 U of SUPERase-In RNase Inhibitor; Ambion). Three independent replicates (50 cells/replicate) per condition were analyzed. RNA/cDNA was obtained and amplified as per the SMARTSEQ2 protocol<sup>5,6</sup>. Libraries were prepared for

sequencing using the Illumina Nextera XT DNA preparation kit. RNA-seq data was generated using a 50 single-end sequencing protocol. Pooled libraries were sequenced on the Illumina HiSeq 4000 platform. Reads were mapped to the human genome (Ensembl 81) and the ERCC sequences using STAR (version 2.4.2a) with default parameters. HTseq-count<sup>7</sup> was used to count the number of reads mapped to each gene with -s no (non-strand specific mode). Data were normalized for sequencing depth using the size factor from the DESeq2 package (version 1.12.2)<sup>8</sup>. Low-input RNA-seq data is deposited and available at GEO (GSE118947).

Bulk RNA-seq data on t(4;11)+ B-ALL patients was generated on the Illumina HiSeq 2500 platform using a 76 paired-end sequencing protocol and aligned to the human reference genome (hg19) using Tophat<sup>19</sup>. A gene was considered differentially expressed in MA4-A4M+ HEPs when it was >2-fold regulated ( $p < 0.01$ ) compared with the equivalent gene in EV-HEPs. Analysis of functional categories and biofunctions was performed with the genes differentially expressed using Ingenuity Pathway Analysis software (Ingenuity Inc., Redwood City, CA). Potential read pairs supporting the expression of MA4 and A4M fusion transcripts in patient samples were identified manually and with in-house written scripts as pairs in which each read aligned unambiguously to a different gene and which were compatible with the genomic breakpoints that were determined at the DNA level in all the samples. Additionally, RT-PCR with primers corresponding to *AF4* exon3 and *MLL* exon 12 (exons contained in all predicted fusions) was performed in all the samples to confirm the expression of any potential isoform of the reciprocal fusion gene. The identity of the isoform was confirmed by capillary sequencing. Finally, the expression of each fusion gene was determined by qRT-PCR using primer pairs spanning the breakpoint between genes. RNA-seq data is deposited and available at GEO (accession number GSE111263).

## SUPPLEMENTARY REFERENCES

1. Guiu J, Bergen DJ, De Pater E, et al. Identification of *Cdca7* as a novel Notch transcriptional target involved in hematopoietic stem cell emergence. *J Exp Med*. 2014;211(12):2411-2423.
2. Li H, Durbin R. Fast and accurate short read alignment with Burrows-Wheeler transform. *Bioinformatics*. 2009;25(14):1754-1760.
3. Zhang Y, Liu T, Meyer CA, et al. Model-based analysis of ChIP-Seq (MACS). *Genome Biol*. 2008;9(9):R137.
4. Welch RP, Lee C, Imbriano PM, et al. ChIP-Enrich: gene set enrichment testing for ChIP-seq data. *Nucleic Acids Res*. 2014;42(13):e105.
5. Picelli S, Bjorklund AK, Faridani OR, Sagasser S, Winberg G, Sandberg R. Smart-seq2 for sensitive full-length transcriptome profiling in single cells. *Nat Methods*. 2013;10(11):1096-1098.
6. Picelli S, Faridani OR, Bjorklund AK, Winberg G, Sagasser S, Sandberg R. Full-length RNA-seq from single cells using Smart-seq2. *Nat Protoc*. 2014;9(1):171-181.
7. Anders S, Pyl PT, Huber W. HTSeq--a Python framework to work with high-throughput sequencing data. *Bioinformatics*. 2015;31(2):166-169.
8. Love MI, Huber W, Anders S. Moderated estimation of fold change and dispersion for RNA-seq data with DESeq2. *Genome Biol*. 2014;15(12):550.

## SUPPLEMENTARY LEGENDS

**Figure S1. Coding sequence of the A4M fusion used in this study. (A)** The full-length cDNA was sequenced-verified. Fusion breakpoint is located in AF4 exon 2 and MLL exon 10. **(B)** Schematic of lentivectors used in this study.

**Figure S2. Co-expression of MA4 and A4M promotes specification rather than survival/proliferation of HEPs. (A)** Day 20 MA4-expressing hEBs display a significant higher HEP production coupled to an impaired blood (CD45<sup>+</sup> and CD45<sup>+</sup>CD34<sup>+</sup>) formation. **(B)** *Left*, representative FACS analysis of the identification of HEPs and CD45<sup>+</sup> hematopoietic cells and their cell-cycle distribution. *Right*, frequency of proliferating (S+G<sub>2</sub>M phases) CD45<sup>+</sup> blood cells and HEPs. **(C)** *Left*, representative FACS analysis of apoptotic CD45<sup>+</sup> hematopoietic cells and HEPs. *Right*, frequency of apoptotic (Annexin V<sup>+</sup>) HEPs and CD45<sup>+</sup> hematopoietic cells for the indicated genotypes.

**Figure S3. H3K79me3 ChIP-seq profiles for the different genotypes. (A)** Correlation heatmap for both H3K79me3 and H3K4me3 using affinity scores based on read counts in consensus peaks distinguishes between the four experimental groups. **(B)** Venn diagrams depicting the number of differentially enriched genomic regions for H3K79me3 between experimental groups relative to EV. **(C)** Quantitative expression of the indicated *HOX-A* genes in CFUs from day 15 EV- and double-fusion-expressing HEPs.

**Figure S4. H3K4me2 profiles at genomic loci of MLL targets identified by Guenther *et al.*** Representative profiles for ChIP-seq using an anti-H3K4me<sup>3</sup> antibody at genomic sites of HOX-A **(A)** and non-HOX **(B)** MLL targets in the indicated genotypes of human ESC-differentiating derivatives.

## Bueno C *et al.* Figure S1

A

AF4-MLL (8739 bp)

Red: AF4 exon 1-3

Blue: MLL exon 10 to 36

ATG :Start Codon

TAA :Stop Codon

ATGGCAGCCCAGTCAAGTTTGTACAATGACGACAGAAACCTGCTTCGAATTAGAGAGAAGGAA  
AGACGCAACCAGGAAGCCCACCAAGAGAAAGAGGCATTTCTGAAAAGATTCCCCTTTTTGGA  
GAGCCCTACAAGACAGCAAAAAGGTGATGAGCTGTCTAGTCGAATACAGAACATGTTGGGAAAC  
TACGAAGAAGTGAAGGAGTTCCCTTAGTACTAAGTCTCACACTCATCGCCTGGATGCTTCTGAAA  
ATAGGTTGGGAAAGCCGAAATATCCTTTAATTCCTGACAAAGGGAGCAGCATTCCATCCAGCT  
CCTTCCACACTAGTGTCCACCACCAGTCCATTACACTCCTGCGTCTGGACCACTTTCTGTTGG  
CAACATTAGCCACAATCCAAAGATGGCGCAGCCAAGAAGTGAACCAATGCCAAGTCTCCATGC  
CAAAGCTGCGGCCACCCGGACAGCCAGCACCTGACCCAGGATCGCCTTGGTCAGGAGGGG  
TTCGGCTCTAGTCATCACAAGAAAGGTGACCGAAGAGCTGACGGAGACCACTGTGCTTCGGT  
GACAGATTGCGCTCCAGAGAGGGAGCTTTCTCCCTTAATCTCTTTGCCTTCCCCAGTTCCCC  
TTTGTACCTATACATTCCAACCAGCAAACCTTTCCCCGGACGCAAGGAAGCAGCAAGGTTCA  
TGGCAGCAGCAATAACAGTAAAGGCTATTGCCAGCCAAATCTCCAAGGACCTAGCAGTGAA  
AGTCCATGATAAAGAGACCCCTCAAGACAGTTTGGTGGCCCCTGCCAGCCGCCTTCTCAGAC  
ATTTCCACCTCCCTCCCTCCCTCAAAAAGTGTGCAATGCAGCAGAAGCCCACGGCTTATGT  
CCGGCCCATGGATGGTCAAGATCAGGCCCTAGTGAATCCCCTGAACTGAAACCACTGCCGG  
AGGACTATCGACAGCAGACCTTTGAAAAACAGACTTGAAAGTGCCTGCCAAAGCCAAGCTCA  
CCAAACTGAAGATGCCTTCTCAGTCAGTTGAGGAGGATTGTGAAGCAGAAAATGTGTGGGAGA  
TGGGAGGCTTAGGAATCTTGACTTCTGTTTCTATAACACCCAGGGTGGTTTGTCTTCTGTGC  
CAGTAGTGGGCATGTAGAGTTTGTGTATTGCCAAGTCTGTTGTGAGCCCTTCCACAAGTTTTGT  
TTAGAGGAGAACGAGCGCCCTCTGGAGGACCAGCTGGAAAATTGGTGTGTCGTCGTTGCAA  
ATTCTGTACGTTTTGTGGAAGGCAACATCAGGCTACAAAGCAGCTGCTGGAGTGAATAAGTG  
CCGAAACAGCTATCACCTGAGTGCCTGGGACCAAACCTACCCACCAAACCCACAAAGAAGAA  
GAAAGTCTGGATCTGTACCAAGTGTGTTTCGCTGTAAGAGCTGTGGATCCACAACCTCCAGGCAA  
AGGGTGGGATGCACAGTGGTCTCATGATTTCTCACTGTGTCATGATTGCGCCAAGCTCTTTGC  
TAAAGGAAACTTCTGCCCTCTCTGTGACAAATGTTATGATGATGATGACTATGAGAGTAAGATG  
ATGCAATGTGGAAAGTGTGATCGCTGGGTCCATTCCAAATGTGAGAATCTTTCAGGTACAGAA  
GATGAGATGTATGAGATTCTATCTAATCTGCCAGAAAGTGTGGCCTACACTTGTGTGAACTGTA  
CTGAGCGGCACCCTGCAGAGTGGCGACTGGCCCTTGAAAAAGAGCTGCAGATTTCTCTGAAG  
CAAGTTCTGACAGCTTTGTTGAATTCTCGGACTACCAGCCATTTGCTACGCTACCGGCAGGCT  
GCCAAGCCTCCAGACTTAAATCCCGAGACAGAGGAGAGTATACCTTCCCGCAGCTCCCCCGA  
AGGACCTGATCCACCAGTTCTTACTGAGGTGAGCAAACAGGATGATCAGCAGCCTTTAGATCT  
AGAAGGAGTCAAGAGGAAGATGGACCAAGGGAATTACACATCTGTGTTGGAGTTTCAAGTATGA  
TATTGTGAAGATCATTCAAGCAGCCATTAATTCAGATGGAGGACAGCCAGAAATTAAGGAGCC  
AACAGCATGGTCAAGTCCCTTCTTTCATTCCGGCAAATGGAACGTGTTTTTCCATGGTTCAAGTGTCA  
AAAAGTCCAGGTTTTGGGAGCCAAATAAAGTATCAAGCAACAGTGGGATGTTACCAAACGCAG  
TGCTTCCACCTTCACTTGACCATAATTATGCTCAGTGGCAGGAGCGAGAGGAAAACAGCCACA  
CTGAGCAGCCTCCTTAATGAAGAAAATCATTCCAGCTCCCAAACCCAAAGGTCTGGAGAAC  
CAGACTACCAAACCTCTCTGCATCCTCTACACCACCAATTTTGGAGTACTGATAGGAGTCGAGA  
AGACAGTCCAGAGCTGAACCCACCCCCAGGCATAGAAGACAATAGACAGTGTGCGTTATGTTT  
GACTTATGGTGTGACAGTGCTAATGATGCTGGTTCGTTTACTATATATTGGCCAAAATGAGTGG

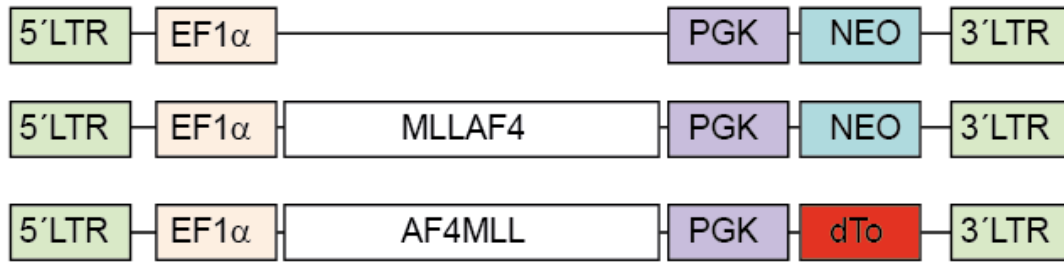
ACACATGTA AATTGTGCTTTGTGGTCAGCGGAAGTGTTTGAAGATGATGACGGATCACTAAAGA  
ATGTGCATATGGCTGTGATCAGGGGCAAGCAGCTGAGATGTGAATTCTGCCAAAAGCCAGGA  
GCCACCGTGGGTTGCTGTCTCACATCCTGCACCAGCAACTATCACTTCATGTGTTCCCGAGCC  
AAGAAGTGTGCTTTCTGGATGATAAAAAAGTATATTGCCAACGACATCGGGATTTGATCAAAG  
GCGAAGTGGTTCCTGAGAATGGATTTGAAGTTTTGAGAAGAGTGTGGACTTTGAAGGAAT  
CAGCTTGAGAAGGAAGTTTCTCAATGGCTTGAACCAGAAAATATCCACATGATGATTGGGTCT  
ATGACAATCGACTGCTTAGGAATTCTAAATGATCTCTCCGACTGTGAAGATAAGCTCTTTCCTAT  
TGGATATCAGTGTTCAGGGTATACTGGAGCACCACAGATGCTCGCAAGCGCTGTGTATATAC  
ATGCAAGATAGTGGAGTGCCGTCTCCAGTCGTAGAGCCGGATATCAACAGCACTGTTGAACA  
TGATGAAAACAGGACCATTGCCCATAGTCCAACATCTTTTACAGAAAAGTTCATCAAAGAGAGT  
CAAACACAGCTGAAATTATAAGTCCTCCATCACCAGACCGACCTCCTCATTACAAAACCTCTG  
GCTCCTGTTATTATCATGTCATCTCAAAGGTCCCAGGATTCGAACACCCAGTTATTCTCCAAC  
ACAGAGATCCCCTGGCTGTGACCGTTGCCTTCTGCAGGAAGTCCTACCCCAACCACTCATGA  
AATAGTCACAGTAGGTGATCCTTTACTCTCCTCTGGACTTCGAAGCATTGGCTCCAGGCGTCA  
CAGTACCTCTTCCTTATCACCCCAGCGGTCCAAACTCCGGATAATGTCTCCAATGAGAAGTGG  
GAATACTTACTCTAGGAATAATGTTTCTCAGTCTCCACCACCGGGACCGCTACTGATCTTGAA  
TCAAGTGCCAAAGTAGTTGATCATGTCTTAGGGCCACTGAATCAAGTACTAGTTTAGGGCAA  
ACACTTCCACCTCTTCAAATTTGCAAAGGACAGTGGTACTGTAGGCAATAAAAACAGTCACTT  
GGATGGATCTTCATCTTCAGAAATGAAGCAGTCCAGTGCCTCAGACTTGGTGTCCAAGAGCTC  
CTCTTTAAAGGGAGAGAAGACCAAAGTGTGAGTTCCAAGAGCTCAGAGGGATCTGCACATAA  
TGTGGCTTACCCTGGAATTCCTAAACTGGCCCCACAGGTTCAACACAACATCTAGAGAAGTGA  
AATGTTAGTAAAATCGGCTCCTTTGCTGAACCCTCTTCAGTGTGTTTTCTTCTAAAGAGGCC  
TCTCCTTCCCACACCTCCATTTGAGAGGGCAAAGGAATGATCGAGACCAACACACAGATTCTA  
CCCAATCAGCAAACCTCCTCTCCAGATGAAGATACTGAAGTCAAACCTTGAAGCTATCTGGAAT  
GAGCAACAGATCATCCATTATCAACGAACATATGGGATCTAGTTCAGAGATAGGAGACAGAA  
AGGGAAAAAATCCTGTAAAGAAAATTTCAAAGAAAAGCATTCCAGTAAATCTTTTTTGAACCTG  
GTCAGGTGACAACCTGGTGAGGAAGGAACTTGAAGCCAGAGTTTATGGATGAGGTTTTGACTC  
CTGAGTATATGGGCCAACGACCATGTAACAATGTTTCTTCTGATAAGATTGGTGATAAAGGCC  
TTCTATGCCAGGAGTCCCCAAAGCTCCACCATGCAAGTAGAAGGATCTGCCAAGGAATTACA  
GGCACCACGGAAACGCACAGTCAAAGTGACACTGACACCTCTAAAAATGGAAAATGAGAGTCA  
ATCCAAAAATGCCCTGAAAGAAAGTAGTCTGCTTCCCCTTTGCAAATAGAGTCAACATCTCCC  
ACAGAACCAATTTAGCCTCTGAAAATCCAGGAGATGGTCCAGTGGCCCAACCAAGCCCCAAT  
AATACCTCATGCCAGGATTCTCAAAGTAACAACATATCAGAATCTTCCAGTACAGGACAGAAACC  
TAATGCTTCCAGATGGCCCCAAACCTCAGGAGGATGGCTCTTTTAAAGGAGGTATCCCCGTC  
GCAGTGGCCGTGCACGTTCTAACATGTTTTTTGGGCTTACCCCACTCTATGGAGTAAGATCCTA  
TGGTGAAGAAGACATTCCATTCTACAGCAGCTCAACTGGGAAGAAGCGAGGCAAGAGATCAGC  
TGAAGGACAGGTGGATGGGGCCGATGACTTAAGCACTTCCAGATGAAGACGACTTATACTATTA  
CAACTTCACTAGAACAGTGATTTCTTCCAGGTGGAGAGGAACGACTGGCATCCATAATTTATTT  
CGGGAGGAGGAACAGTGTGATCTTCCAAAAATCTCACAGTTGGATGGTGTGATGATGGGACA  
GAGAGTGATACTAGTGTACAGCCACAACAAGGAAAAGCAGCCAGATTCCAAAAAGAAATGGT  
AAAGAAAATGGAACAGAGAACTTAAAGATTGATAGACCTGAAGATGCTGGGGAGAAAGAACAT  
GTCATAAGAGTTCTGTTGGCCACAAAAATGAGCCAAAGATGGATAACTGCCATTCTGTAAGCA  
GAGTTAAAACACAGGGACAAGATTCTTGAAGCTCAGCTCAGCTCATTGGAGTCAAGCCGCA  
GAGTCCACACAAGTACCCCTCCGACAAAAATTTACTGGACACCTATAATACTGAGCTCCTGAA  
ATCAGATTCAGACAATAACAACAGTGTGACTGTGGGAATATCCTGCCTTCCAGACATTATGGAC  
TTTGTACTAAAGAATACTCCATCCATGCAGGCTTTGGGTGAGAGCCCAGAGTCATCTTCATCAG  
AACTCCTGAATCTTGGTGAAGGATTGGGTCTTGACAGTAATCGTGA AAAAGACATGGGTCTTTT  
TGAAGTATTTTCTCAGCAGCTGCCTACAACAGAACCTGTGGATAGTAGTGTCTCTTCTCTATC  
TCAGCAGAGGAACAGTTTGGAGTTGCCTCTAGAGCTACCATCTGATCTGTCTGTCTTGACCACC  
CGGAGTCCCCTGTCCCCAGCCAGAATCCCAGTAGACTAGCTGTTATCTCAGACTCAGGGGA  
GAAGAGAGTAACCATCACAGAAAAATCTGTAGCCTCCTCTGAAAGTGACCCAGCACTGCTGAG  
CCCAGGAGTAGATCCAACCTCTGAAGGCCACATGACTCCTGATCATTTTATCCAAGGACACAT



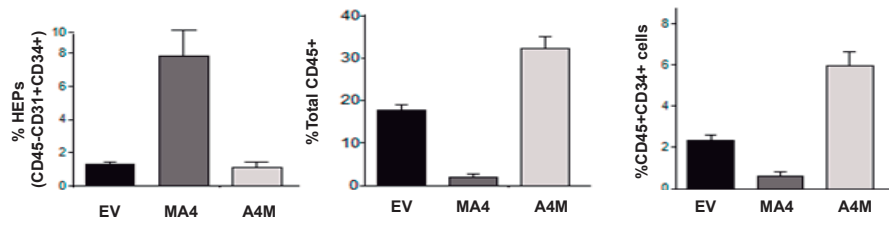
GGATGCAGACCACATCTCTAGCCCTCCTTGTGGTTCAGTAGAGCAAGGTCATGGCAACAATCA  
GGATTTAACTAGGAACAGTAGCACCCCTGGCCTTCAGGTACCTGTTTCCCCAACTGTTCCCAT  
CCAGAACCAGAAGTATGTGCCCAATTCTACTGATAGTCCTGGCCCGTCTCAGATTTCCAATGCA  
GCTGTCCAGACCACTCCACCCACCTGAAGCCAGCCACTGAGAACTCATAGTTGTTAACCAG  
AACATGCAGCCACTTTATGTTCTCCAACTCTTCCAAATGGAGTGACCCAAAAAATCCAATTGA  
CCTCTTCTGTTAGTTCTACACCCAGTGTGATGGAGACAAATACTTCAGTATTGGGACCCATGGG  
AGGTGGTCTCACCCTTACCACAGGACTAAATCCAAGCTTGCCAACTTCTCAATCTTTGTTCCCT  
TCTGCTAGCAAAGGATTGCTACCCATGTCTCATCACCCAGCACTTACATTCCCTCCCTGCAGCTA  
CTCAAAGTAGTTTCCCACCAAACATCAGCAATCCTCCTTCAGGCCTGCTTATTGGGGTTCAGCC  
TCCTCCGGATCCCCAACTTTTGGTTTTCAGAATCCAGCCAGAGGACAGACCTCAGTACCACAGT  
AGCCACTCCATCCTCTGGACTCAAGAAAAGACCCATATCTCGTCTACAGACCCGAAAGAATAAA  
AACTTGCTCCCTCTAGTACCCCTTCAAACATTGCCCTTCTGATGTGGTTTCTAATATGACATT  
GATTAACCTTCACACCCTCCCAGCTTCCCTAATCATCCAAGTCTGTTAGATTTGGGGTCACTTAATA  
CTTCATCTCACCGAACTGTCCCCAACATCATAAAAAGATCTAAATCTAGCATCATGTATTTTGAA  
CCGGCACCCCTGTTACCACAGAGTGTGGGAGGAACTGCTGCCACAGCGGCAGGCACATCAAC  
AATAAGCCAGGATACTAGCCACCTCACATCAGGGTCTGTGTCTGGCTTGGCATCCAGTTCCTC  
TGTCTTGAATGTTGTATCCATGCAAACCTACCACAACCCCTACAAGTAGTGCGTCAGTTCAGGA  
CACGTACCTTAACCAACCCAAGGTTGCTTGGTACCCAGATATTGGCTCAATAAGCAATCTTT  
TAATCAAAGCTAGCCAGCAGAGCCTGGGGATTACAGGACCAGCCTGTGGCTTTACCGCCAAGTT  
CAGGAATGTTTCCACAACCTGGGGACATCACAGACCCCTCTACTGCTGCAATAACAGCGGCAT  
CTAGCATCTGTGTGCTCCCTCCACTCAGACTACGGGCATAACAGCCGCTTACCTTCTGGGG  
AAGCAGACGAACACTATCAGCTTCAGCATGTGAACCAGCTCCTTGCCAGCAAACTGGGATTC  
ATTCTTCCCAGCGTGATCTTGATTCTGCTTCAGGGCCCCAGGTATCCAACCTTACCCAGACGGT  
AGACGCTCCTAATAGCATGGGACTGGAGCAGAACAAGGCTTTATCCTCAGCTGTGCAAGCCAG  
CCCCACCTCTCCTGGGGTCTCCATCCTCTCCATCTTCTGGACAGCGGTGAGCAAGCCCTTC  
AGTGCCGGGTCCCACTAAACCCAAACCAAAAACCAACCGTTTTAGCTGCCTCTAGACAAAGG  
GAATGGCAAGAAGCACAATGTTTCCCATTTGCGGACCAGTTCTTCTGAAGCACACATTCCAGA  
CCAAGAAACGACATCCCTGACCTCAGGCACAGGGACTCCAGGAGCAGAGGCTGAGCAGCAG  
GATACAGCTAGCGTGGAGCAGTCTCCAGAAAGGAGTGTGGGCAACCTGCAGGGCAAGTCGC  
TGTTCTTCCGGAAGTTCAGGTGACCCAAAATCCAGCAAATGAACAAGAAAGTGCAGAACCTAA  
AACAGTGAAGAAGAGGAAAGTAATTTAGCTCCCACTGATGCTTTGGCTTCAGCAAGAACA  
AAAGCGGAAGGAAAGCATTACTGAGAAAAAACCAAGAAAGGACTTGTTTTTGAATTTCCAGT  
GATGATGGCTTTAGATCTGTGCAGAAAGTATTGAAGATGCCTGGAAGTCATTGACAGATAAAG  
TCCAGGAAGCTCGATCAAATGCCCGCCTAAAGCAGCTCTCATTTGCAGGTGTTAACGGTTTGA  
GGATGCTGGGGATTCTCCATGATGCAGTTGTGTTCCCTCATTGAGCAGCTGTCTGGTGCCAAGC  
ACTGTCGAAATTACAAATTCGTTTTCCACAAGCCAGAGGAGGCAATGAACCCCTTGAACC  
CTCACGGCTCAGCCAGGGCTGAAGTCCACCTCAGGAAGTCAGCATTTGACATGTTAACTTCC  
TGGCTTCTAAACATCGTCAGCCTCCTGAATACAACCCCAATGATGAAGAAGAGGAGGAGGTAC  
AGCTGAAGTCAGCTCGGAGGGCAACTAGCATGGATCTGCCAATGCCCATGCGCTTCCGGCAC  
TTAAAAAAGACTTCTAAGGAGGCAGTTGGTGTCTACAGGTCTCCCATCCATGGCCGGGGTCTT  
TTCTGTAAGAGAAACATTGATGCAGGTGAGATGGTATTGAGTATGCCGGCAACGTCATCCGC  
TCCATCCAGACTGACAAGCGGGAAAAGTATTACGACAGCAAGGGCATTGGTTGCTATATGTTCC  
CGAATTGATGACTCAGAGGTAGTGGATGCCACCATGCATGGAAATGCTGCACGCTTCATCAAT  
CACTCGTGTGAGCCTAACTGCTATTCTCGGGTCATCAATATTGATGGGCAGAAGCACATTGTCA  
TCTTTGCCATGCGTAAGATCTACCGAGGAGAGGAACTCACTTACGACTATAAGTTCCCCATTGA  
GGATGCCAGCAACAAGCTGCCCTGCAACTGTGGCGCTAAGAAATGCCGGAAGTTCCTAAAC

A

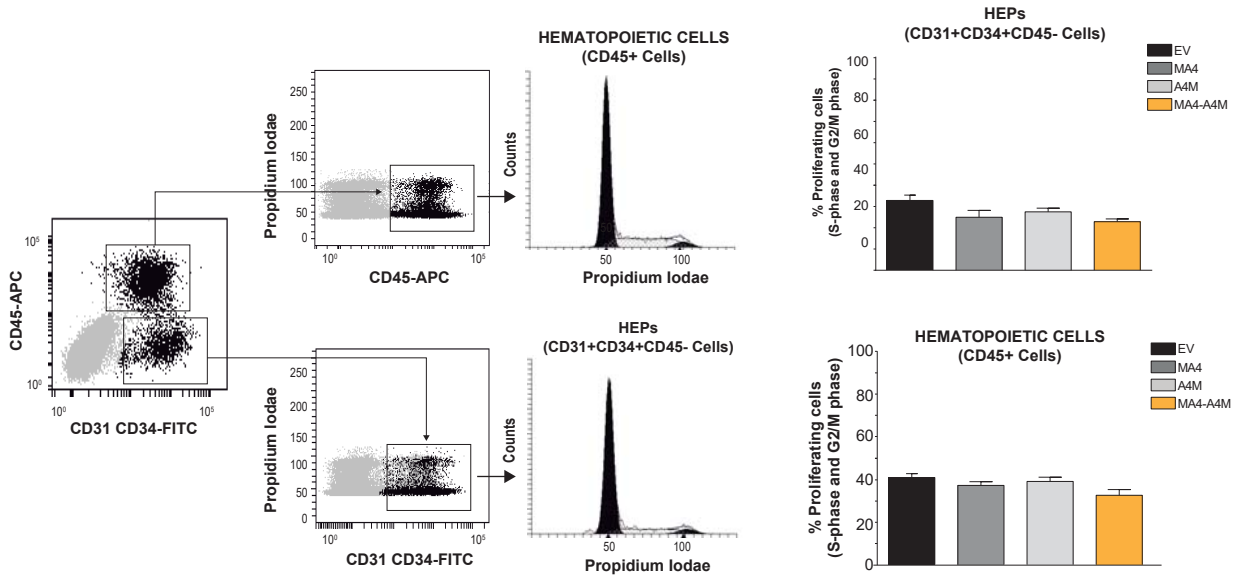
**B**



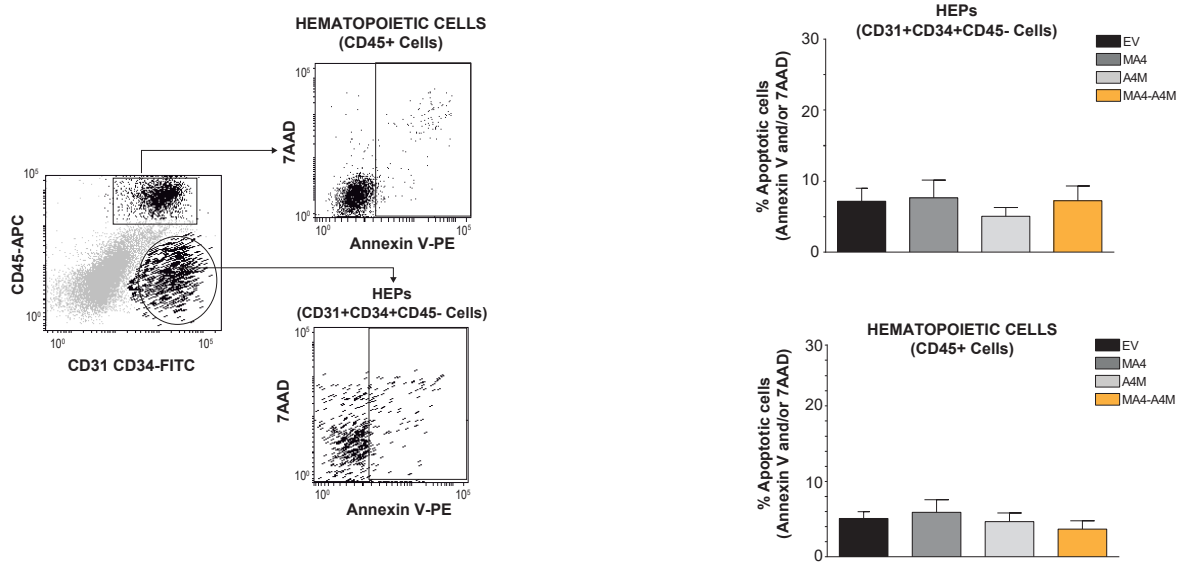
**A**



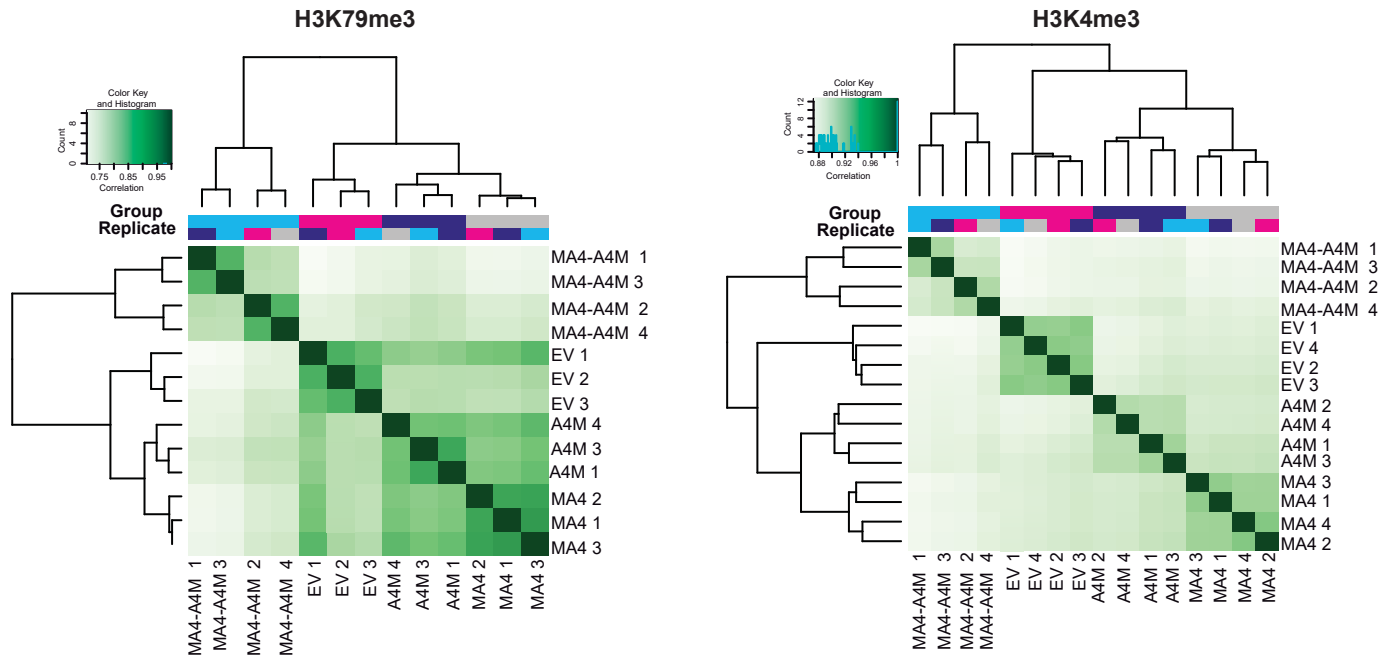
**B**



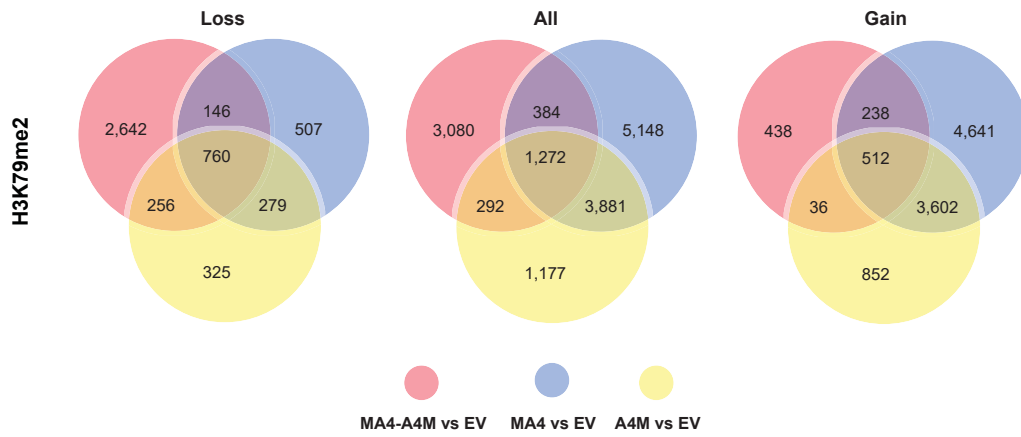
**C**



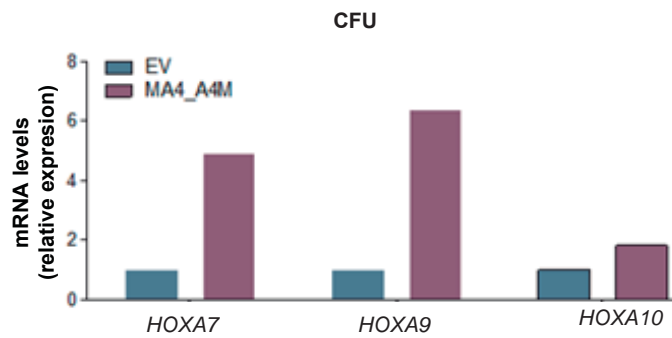
**A**



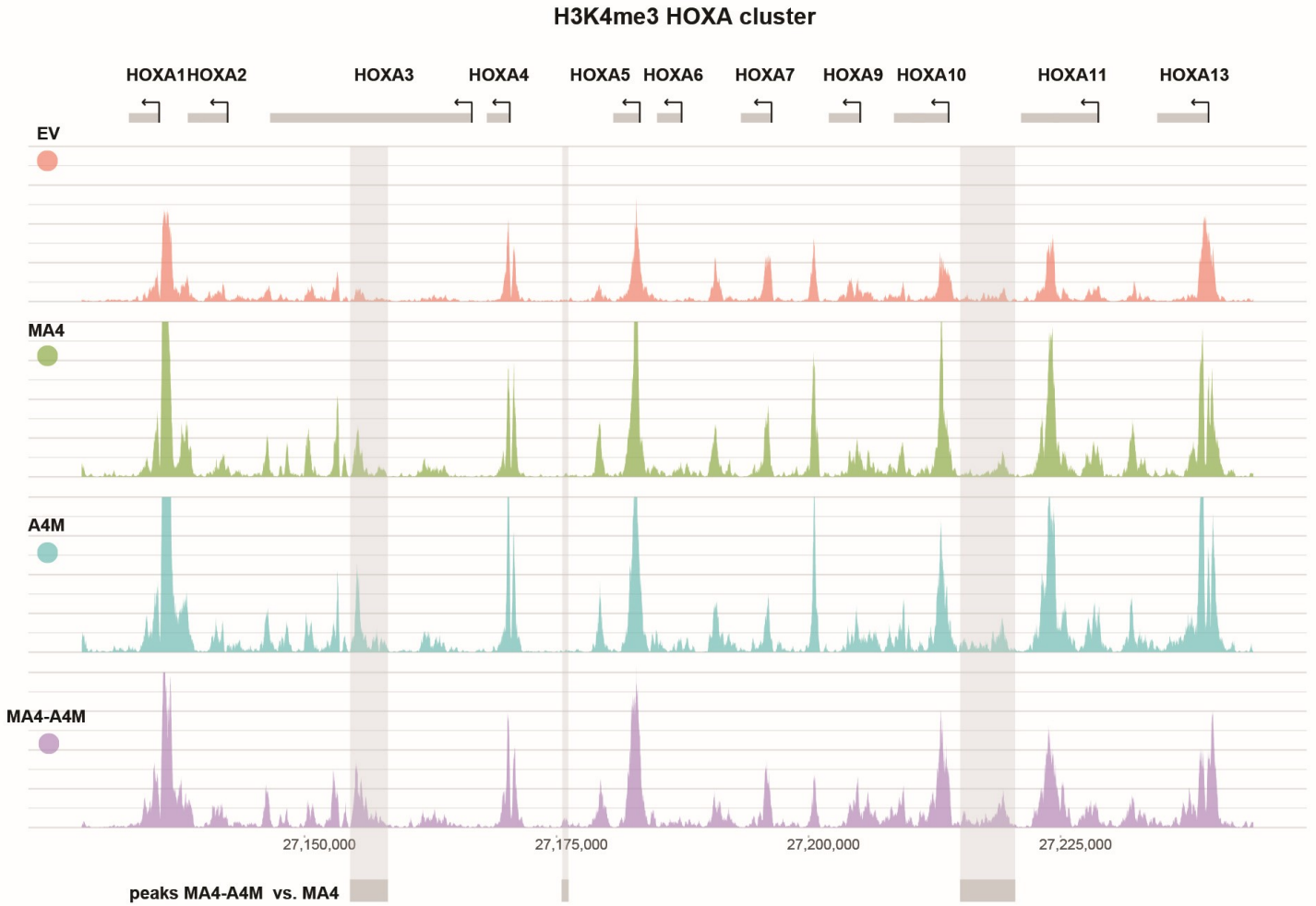
**B**



**C**



**A**



**B**

